AD NUMBER

ADB259838

NEW LIMITATION CHANGE

TO

Approved for public release, distribution unlimited

FROM

Distribution authorized to U.S. Gov't. agencies only; Proprietary Info.; Oct 99. Other requests shall be referred to U.S. Army Medical Research and Materiel Command, 504 Scott St., Fort Detrick, MD 21702-5012.

AUTHORITY

U.S. Army Medical Research and Materiel Command and Fort Detrick ltr., dtd October 17, 2001.

AD_____

Award Number: DAMD17-96-1-6323

TITLE: Role of the EGF-Related Growth Factor *Cripto* in Murine Mammary Tumorigenesis

PRINCIPAL INVESTIGATOR: Michael M. Shen, Ph.D.

CONTRACTING ORGANIZATION: University of Medicine and Dentistry of New Jersey
Robert Wood Johnson Medical School
Piscataway, New Jersey 08854

REPORT DATE: October 1999

TYPE OF REPORT: Annual

PREPARED FOR: U.S. Army Medical Research and Materiel Command
Fort Detrick, Maryland 21702-5012

NOTICE

USING GOVERNMENT DRAWINGS, SPECIFICATIONS, OR OTHER DATA INCLUDED IN THIS DOCUMENT FOR ANY PURPOSE OTHER THAN GOVERNMENT PROCUREMENT DOES NOT IN ANY WAY OBLIGATE THE U.S. GOVERNMENT. THE FACT THAT THE GOVERNMENT FORMULATED OR SUPPLIED THE DRAWINGS, SPECIFICATIONS, OR OTHER DATA DOES NOT LICENSE THE HOLDER OR ANY OTHER PERSON OR CORPORATION; OR CONVEY ANY RIGHTS OR PERMISSION TO MANUFACTURE, USE, OR SELL ANY PATENTED INVENTION THAT MAY RELATE TO THEM.

LIMITED RIGHTS LEGEND

Award Number: DAMD17-96-1-6323
Organization: University of Medicine and Dentistry of New Jersey
Robert Wood Johnson Medical School

Those portions of the technical data contained in this report marked as limited rights data shall not, without the written permission of the above contractor, be (a) released or disclosed outside the government, (b) used by the Government for manufacture or, in the case of computer software documentation, for preparing the same or similar computer software, or (c) used by a party other than the Government, except that the Government may release or disclose technical data to persons outside the Government, or permit the use of technical data by such persons, if (i) such release, disclosure, or use is necessary for emergency repair or overhaul or (ii) is a release or disclosure of technical data (other than detailed manufacturing or process data) to, or use of such data by, a foreign government that is in the interest of the Government and is required for evaluational or informational purposes, provided in either case that such release, disclosure or use is made subject to a prohibition that the person to whom the data is released or disclosed may not further use, release or disclose such data, and the contractor or subcontractor or subcontractor asserting the restriction is notified of such release, disclosure or use. This legend, together with the indications of the portions of this data which are subject to such limitations, shall be included on any reproduction hereof which includes any part of the portions subject to such limitations.

THIS TECHNICAL REPORT HAS BEEN REVIEWED AND IS APPROVED FOR PUBLICATION.

N Mangla current Name
10/28/00

_____

_____

_____

REPORT DOCUMENTATION PAGE

Form Approved
OMB No. 074-0188

1. AGENCY USE ONLY (Leave blank)	2. REPORT DATE	3. REPORT TYPE AND DATES COVERED
	October 1999	Annual (23 Sep 98 - 22 Sep 99)

4. TITLE AND SUBTITLE
Role of the EGF-Related Growth Factor *Cripto* in Murine Mammary Tumorigenesis

5. FUNDING NUMBERS
DAMD17-96-1-6323

6. AUTHOR(S)
Michael M. Shen, Ph.D.

7. PERFORMING ORGANIZATION NAME(S) AND ADDRESS(ES)
University of Medicine and Dentistry of New Jersey
Robert Wood Johnson Medical School
Piscataway, New Jersey 08854

E-Mail:
mshen@cabm.rutgers.edu

8. PERFORMING ORGANIZATION REPORT NUMBER

9. SPONSORING / MONITORING AGENCY NAME(S) AND ADDRESS(ES)
U.S. Army Medical Research and Materiel Command
Fort Detrick, Maryland 21702-5012

10. SPONSORING / MONITORING AGENCY REPORT NUMBER

11. SUPPLEMENTARY NOTES

12a. DISTRIBUTION / AVAILABILITY STATEMENT
Distribution authorized to U.S. Government agencies only (proprietary information, Oct 99). Other requests for this document shall be referred to U.S. Army Medical Research and Materiel Command, 504 Scott Street, Fort Detrick, Maryland 21702-5012.

12b. DISTRIBUTION CODE

13. ABSTRACT *(Maximum 200 Words)*

We have been investigating the biological and biochemical functions of the *Cripto* gene, which encodes an extracellular protein that is a member of the *EGF-CFC* gene family, and which has been implicated in autocrine or paracrine signaling during human breast carcinogenesis. To elucidate the potential role of *Cripto* in mammary development and tumorigenesis, we have been investigating the *in vivo* activities of *Cripto* using transgenic mice that overexpress *Cripto* in the mammary gland, and have been investigating the molecular mechanisms of CRIPTO protein signaling. In the past year, we have generated molecular genetic and biochemical lines of evidence that *Cripto* acts as an essential co-factor for signaling by the divergent TGF-β factor *Nodal*. These findings provide a model for potential mechanisms of *Cripto* function through modulation of specific TGF-β-related signals in mammary development and tumorigenesis.

14. SUBJECT TERMS
(1) growth factor receptor, (2) mammary gland development, (3) transgenic mice, (4) in situ hybridization, (5) cell culture, (6) histochemical affinity reagent

15. NUMBER OF PAGES
26

16. PRICE CODE

17. SECURITY CLASSIFICATION OF REPORT	18. SECURITY CLASSIFICATION OF THIS PAGE	19. SECURITY CLASSIFICATION OF ABSTRACT	20. LIMITATION OF ABSTRACT
Unclassified	Unclassified	Unclassified	Limited

FOREWORD

Opinions, interpretations, conclusions and recommendations are those of the author and are not necessarily endorsed by the U.S. Army.

MW Where copyrighted material is quoted, permission has been obtained to use such material.

MW Where material from documents designated for limited distribution is quoted, permission has been obtained to use the material.

MW Citations of commercial organizations and trade names in this report do not constitute an official Department of Army endorsement or approval of the products or services of these organizations.

✓ In conducting research using animals, the investigator(s) adhered to the "Guide for the Care and Use of Laboratory Animals," prepared by the Committee on Care and use of Laboratory Animals of the Institute of Laboratory Resources, national Research Council (NIH Publication No. 86-23, Revised 1985).

NA For the protection of human subjects, the investigator(s) adhered to policies of applicable Federal Law 45 CFR 46.

NA In conducting research utilizing recombinant DNA technology, the investigator(s) adhered to current guidelines promulgated by the National Institutes of Health.

NA In the conduct of research utilizing recombinant DNA, the investigator(s) adhered to the NIH Guidelines for Research Involving Recombinant DNA Molecules.

MW In the conduct of research involving hazardous organisms, the investigator(s) adhered to the CDC-NIH Guide for Biosafety in Microbiological and Biomedical Laboratories.

[signature] 10/21/99

PI - Signature Date

Table of Contents:

5. Introduction:

Our work on breast development and tumorigenesis has focused on the *Cripto* gene, which encodes an extracellular protein that is a member of the *EGF-CFC* gene family. Previous studies have suggested that *Cripto* may be involved in autocrine or paracrine signaling during human breast carcinogenesis (reviewed in [1]). Thus, *Cripto* is consistently overexpressed in a large percentage of human breast cancers, and is not expressed at high levels in normal breast tissue [2], and *Cripto* has transforming activity when overexpressed in NOG-8 mouse mammary epithelial cells [3]. To elucidate the potential role of *Cripto* in breast development and tumorigenesis, we have been investigating the activities of *Cripto* in mammary development using transgenic mice and cell culture systems, and have been investigating the molecular mechanisms of CRIPTO protein action, with the objective of identifying a putative CRIPTO receptor(s).

6. Body:

In the past year, we have made significant progress towards understanding the molecular mechanisms of *Cripto* function, which has led to an important revision of our initial view of *Cripto* encoding an EGF (epidermal growth factor)-related growth factor. Based on recent molecular genetic data from our lab and others, it now appears that *Cripto* acts as an essential co-factor for signaling by a divergent member of the TGF-β (transforming growth factor-beta) superfamily.

6.a. Review of recent work relevant for our studies

To understand the biological and biochemical basis for *Cripto* function, we have been investigating its role in normal development. We initially identified the *EGF-CFC* family through studies of mesoderm formation during mouse gastrulation, in which we isolated a novel gene that we named *Cryptic* ([4]; see appendix), based on its similarity to murine and human *Cripto* [5, 6]. Mammalian *Cryptic* and *Cripto,* frog *FRL-1,* and zebrafish *oep* encode extracellular proteins [4, 7] that share an N-terminal signal sequence, a variant EGF-like motif, a novel conserved cysteine-rich domain (that we named the CFC (*Cripto, Frl-1,* and *Cryptic*) motif), and a C-terminal hydrophobic region (Fig. 1). Although the overall level of sequence conservation is relatively low (approximately 30% identity), all *EGF-CFC* family members appear to have functionally similar activities in assays for phenotypic rescue of *oep* mutant fish embryos by mRNA microinjection [8].

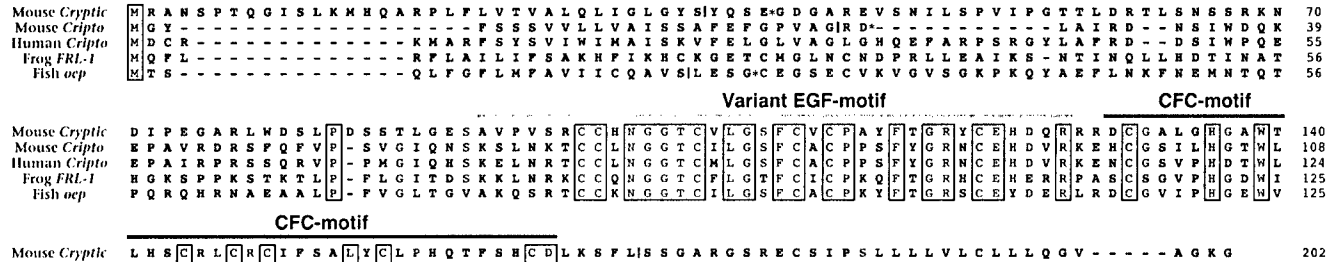

Figure 1. Sequence alignment of EGF-CFC family members. Amino acid residues conserved among all family members are boxed, while residues conserved among four out of five members are shaded. The positions of the variant EGF-motif and the novel CFC motif are indicated. Locations of the predicted sites for N-terminal signal sequence cleavage are indicated by vertical bars; asterisks denote the positions of the N-terminal epitope tag used in expression constructs for mouse *Cripto* and *Cryptic.* Shaded bars indicate the positions of C-terminal truncations constructed for EGF-CFC proteins.

In our work, we have gained essential insights into the biological functions and potential biochemical activities of EGF-CFC proteins through analysis of knock-out mice for *Cripto* and *Cryptic*. We have found that the roles of *EGF-CFC* genes in axis formation are neatly divided in the mouse embryo, so that *Cripto* is required for correct orientation of the A-P (anterior-posterior) axis, while *Cryptic* is necessary for determination of the L-R (left-right) axis ([9, 10]; see appendix). These recent studies have led to a revised model for the biochemical activities of EGF-CFC proteins.

Thus, in contrast to previous models of CRIPTO protein having growth factor activity (reviewed in [1]), recent lines of evidence from molecular genetic studies indicate that EGF-CFC proteins act as essential co-factors for a signaling factor known as NODAL. The *Nodal* gene encodes a signaling factor that is a divergent member of the TGF-β superfamily, and displays a mutant phenotype similar to that for *Cripto* [11, 12]. The downstream signaling pathway for *Nodal* has primarily been suggested by our current understanding of TGF-β signal transduction pathways (reviewed in [13]), and by gene targeting experiments in mice that have demonstrated similar and/or synergistic phenotypes for targeted disruption of *Nodal,* the type II activin receptor *ActRIIB,* the type I receptor *ActR1B,* and the cytoplasmic signal transducer *Smad2* [12, 14-18]; however, there is no biochemical evidence at present that NODAL protein directly binds to and activates activin receptors. Recent work has led to the proposal that NODAL and EGF-CFC proteins are inactive by themselves, while in combination their activity is similar to that of activin [8]. Moreover, the phenotypes of both *Cripto* and *Cryptic* mutant mice can be readily interpreted as resulting from defects in *Nodal* signaling [9, 10]. These data can be summarized in terms of a possible regulatory pathway for *Nodal* and *EGF-CFC* activities (Fig. 2).

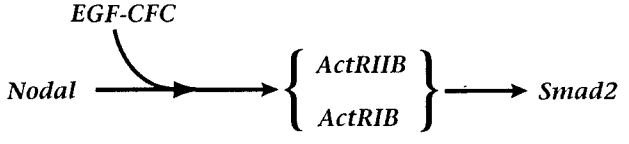

Figure 2. Potential regulatory relationship of *EGF-CFC* activities to the *Nodal* signal transduction pathway. Note that these arrows and bars do not imply direct biochemical interactions. It is important to note, however, that this pathway does not exclude the possibilities that EGF-CFC proteins could act as co-factors for other members of the TGF-β superfamily, or could also act through an unrelated signaling pathway.

These apparently discrepant findings can be resolved by a simple model in which EGF-CFC proteins form membrane-associated components of a receptor complex, and mediate *Nodal* signaling through signal-transducing partner(s) that may include activin receptors [8]. However, in principle, release of EGF-CFC proteins from the membrane might result in a freely diffusible protein, which could form part of a receptor complex on a neighboring cell that may not itself express the *EGF-CFC* gene, in effect acting as a signal. Such a mechanism has been shown to be the case with the GFRα protein, which is tethered to the membrane via a glycosyl-phosphatidylinositol (GPI) linkage and heterodimerizes with the c-RET tyrosine kinase receptor to form a receptor for GDNF, another distant member of the TGF-β superfamily [19, 20]. In this view, the downstream signaling effects documented for CRIPTO protein might represent cross-talk between EGF receptor and SMAD2 signaling pathways, which has been previously documented [21, 22].

6.b. Technical Objective I: Generation and analysis of *Cripto* transgenic mice

Rationale: To investigate the effects of *Cripto* on mammary development and oncogenesis, we have generated transgenic mice that overexpress *Cripto* in the mammary epithelium. Our previous studies had shown that *Cripto* is expressed at extremely low levels throughout mammary development, with slightly elevated expression during pregnancy and lactation. To overexpress *Cripto,* we have produced a modified *Cripto* transgene that should direct high-level secretion. We have previously shown that EGF-CFC proteins, including CRIPTO, are poorly secreted from

transfected cells in culture, probably because the endogenous signal sequence is non-conventional and directs inefficient secretion ([4]; data not shown). Moreover, CRIPTO protein appears to be membrane-associated due to the presence of the C-terminal hydrophobic region (see below). Since the biological activity of a *Cripto* transgene should depend upon the levels of protein secretion attained *in vivo*, we have constructed a transgene expression vector containing a heterologous efficient signal sequence and encoding a C-terminally truncated protein.

Results: To direct expression of CRIPTO transgenes to the mammary epithelium of transgenic mice, we utilized the *MMTV-SVPA* vector [23], which contains a mouse mammary tumor virus (MMTV) long terminal repeat (LTR) enhancer/promoter (Fig. 3a). We have subcloned a modified mouse *Cripto* cDNA (sec-*Cripto*) into this vector (Fig. 3b). We have successfully generated five founder mice carrying this MMTV-sec-*Cripto* transgene, and have established stable lines from each of these founders.

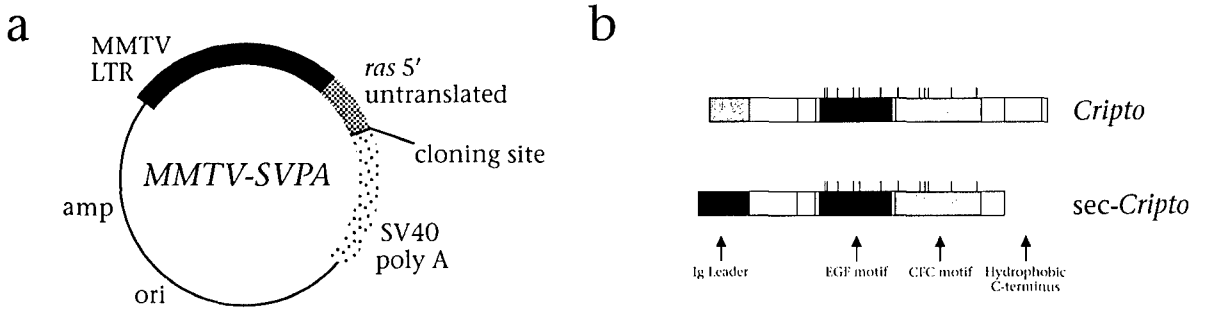

Figure 3. Schematic depiction of the transgene vector and inserts. ***a,*** The *MMTV-SVPA* expression vector contains the long terminal repeat from the mouse mammary tumor virus, 5' untranslated sequences from *ras,* and the 3' polyadenylation region from SV40 [23]. ***b,*** The murine *Cripto* transgene inserts have been produced in unmodifed and modified (Sec-*Cripto*) forms. For the modified construct, we have utilized the leader peptide from a murine immunoglobulin kappa chain gene (from the *pSecTagB* expression vector; Invitrogen) as a replacement for the endogenous CRIPTO leader peptide.

To analyze these transgenic lines, we have examined transgene expression and phenotype at different stages of mammary development, thereby accomplishing tasks 1-5 of our Statement of Work. Four of the five MMTV-sec-*Cripto* transgenic lines display transgene expression in the mammary gland in virgin female animals as well as during pregnancy and lactation (data not shown). However, examination of whole-mounts of mammary fat pads from adult transgenic females revealed no phenotypic abnormalities in virgin, pregnant, lactating, or involuting animals (data not shown). At present, the absence of any detectable phenotype suggests that *Cripto* expression alone is not sufficient to alter mammary epithelial differentiation. We are continuing to monitor these MMTV-sec-*Cripto* mice to determine whether they will develop a mammary phenotype with advancing age or multi-parous status.

These results are consistent with our model that EGF-CFC proteins act as essential co-factors for *Nodal* signaling, and with the finding that broad ectopic overexpression of *oep* in fish did not result in embryonic phenotypes [7]. Our current interpretation is that the ectopic expression of *Cripto* in human breast tumors may reflect a cooperative interaction with overexpressed members of the TGF-β family, perhaps including *Nodal* or related genes. To test this hypothesis, we are now attempting to generate MMTV-*Nodal* transgenic mice, and to cross these mice with the MMTV-sec-*Cripto* transgenics to examine the resulting phenotype.

[redacted]/UNPUBLISHED DATA

6.c. Technical Objective II: Expression of *Cripto* in cell culture model systems

Rationale: To examine the role of *Cripto* in cellular proliferation, differentiation and transformation, we have been utilizing retroviral gene transfer as a strategy to efficiently transfect *Cripto* into relevant cell lines. In studies reported in the previous update, we have focused on cell lines that have been reported to respond to exogenous human CRIPTO protein, such as the HC-11 mammary epithelial cell line [24, 25], and have made significant progress towards tasks 8-10.

Based on the apparent lack of phenotype of the MMTV-sec-*Cripto* transgenic mice, however, we have decided not to continue our experiments on mammary cell lines until we have acquired a better understanding of the biochemical basis of CRIPTO protein function. We are currently undertaking a survey of expression of *Nodal* and closely related TGF-β factors (such as *Vg1*) in a range of mammary cell lines, with the expectation that expressing cell lines will be more likely to display phenotypic changes in response to *Cripto* expression. These experiments will provide the preliminary data necessary to test the hypothesis that co-expression of *Cripto* with specific TGF-β factors may play a critical role in mammary differentiation and/or tumorigenesis.

6.d. Technical Objective III: Biochemical analysis of CRIPTO function

Rationale: Despite the present lack of understanding as to the potential mechanism(s) by which *EGF-CFC* and *Nodal* activities might interact at the molecular level, understanding the biochemical basis of this interaction is of fundamental importance. Therefore, we have undertaken to *(i)* characterize the cellular localization of CRIPTO protein, *(ii)* produce and purify active CRIPTO protein for biochemical analyses, and *(iii)* examine potential interactions between CRIPTO and NODAL proteins. These experiments form the basis for elucidating the biochemical mechanism of CRIPTO function.

Results: ***(i) Membrane-association of CRIPTO protein:*** Previous studies have suggested that members of the *EGF-CFC* family encode extracellular proteins that are localized to the surface of transfected cells, with this association mediated by the C-terminal hydrophobic domain [4, 7]. Therefore, we have investigated whether CRIPTO is in fact a secreted protein that is membrane-associated. Our previous work had demonstrated that CRYPTIC protein underwent signal sequence cleavage and N-linked glycosylation when expressed by *in vitro* transcription/translation in the presence of microsomal membranes [4]. However, since the C-termini of EGF-CFC proteins are not conserved in their amino acid sequences, but only in their hydrophobicity (Fig. 1), it was unclear whether mammalian CRIPTO and would be membrane-associated via its C-terminus, as has been shown for Oep protein [7]. Moreover, in previous experiments using alkaline phosphatase-CRYPTIC fusion proteins, we had detected very low levels of fusion protein in culture supernatants of transfected COS cells [4].

To determine whether CRIPTO protein is indeed secreted and membrane-associated, we investigated its cellular localization in transfected mammalian cells using immunofluorescence detection of epitope-tagged proteins (data not shown), and obtained results similar to that described for Oep [7]. Furthermore, we have extended these findings by cellular fractionation experiments, using insect cells infected with baculoviruses expressing a secreted CRIPTO protein fused at its N-terminus to glutathione-S-transferase (GST) (Fig. 4). In this experiment, we found that purified plasma membrane fractions contained both full-length and C-terminal truncations of the GST-CRIPTO fusion protein, as detected by Western blotting using a specific anti-CRIPTO antiserum. In contrast, the culture supernatants from infected cells contained high levels of the truncated protein, but only barely detectable levels of the full-length protein. These results support the idea that full-length EGF-CFC proteins are associated with the cell membrane, while C-terminal

truncated proteins can be secreted into culture supernatants. At present, however, it remains unclear whether full-length EGF-CFC proteins remain associated with the cell surface through a C-terminal transmembrane domain, through tight association with other membrane proteins, or through a lipophilic modification.

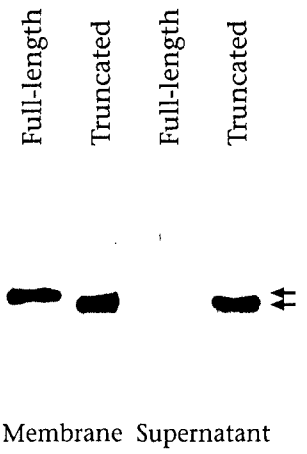

Figure 4. Western blot detection of CRIPTO protein in plasma membrane fractions and culture supernatants prepared from baculovirus-infected insect cells. Arrows at right indicate positions of full-length and truncated GST-CRIPTO fusion proteins. **Methods.** For expression of secreted GST-CRIPTO fusion proteins, *Cripto* cDNAs corresponding to the mature protein with an intact or truncated C-terminus (as shown in Fig. 2) were cloned into the *pAcSecG2T* transfer vector (Pharmingen), which contains a *gp67* signal sequence for high-level secretion, and generates an N-terminal fusion with GST. Baculovirus stocks were prepared in Sf9 insect cells and used to infect High-5 insect cells (Invitrogen). Plasma membrane fractionation was performed essentially as described [26, 27]. The absence of contaminating endoplasmic reticulum in the plasma membrane fractions was confirmed using assays for cytochrome b_5 reductase (not shown). Rabbit polyclonal antisera specific for CRIPTO were generated (Covance) by immunization with GST-CRIPTO fusion proteins expressed in *E. coli* and purified using glutathione-agarose beads. The antisera were characterized for specificity in Western blotting experiments using EGF-CFC proteins expressed in bacterial and mammalian cells.

(ii) Expression of active CRIPTO protein in insect cells: To achieve expression of active CRIPTO protein, we employed a baculovirus expression strategy that would result in secretion of CRIPTO into the culture supernatant of infected insect cells. For this purpose, we utilized the *pMelBac* baculovirus transfer vector (Invitrogen), which contains a heterologous signal sequence, to express C-terminally truncated CRIPTO protein (without epitope tags) at high levels in culture supernatants. To enable rapid and efficient protein purification, we infected High-5 insect cells (Invitrogen) grown in defined serum-free media; by adjusting the time course and multiplicity of infection, we determined optimal conditions for harvesting culture supernatants to minimize contamination from cytoplasmic proteins released by lysed cells We were able to achieve efficient purification of CRIPTO from culture supernatants using a Sephadex G-75 gel filtration column (Fig. 5a). As shown in Fig. 5b,c, we were able to obtain at least 90% pure CRIPTO protein in specific column fractions, as judged by examination of silver stained gels and by Western blotting using a specific CRIPTO polyclonal antisera. In subsequent experiments, we have scaled-up the purification protocol and have obtained approximately 400 µg of purified CRIPTO protein from 1 liter of insect cell culture supernatants.

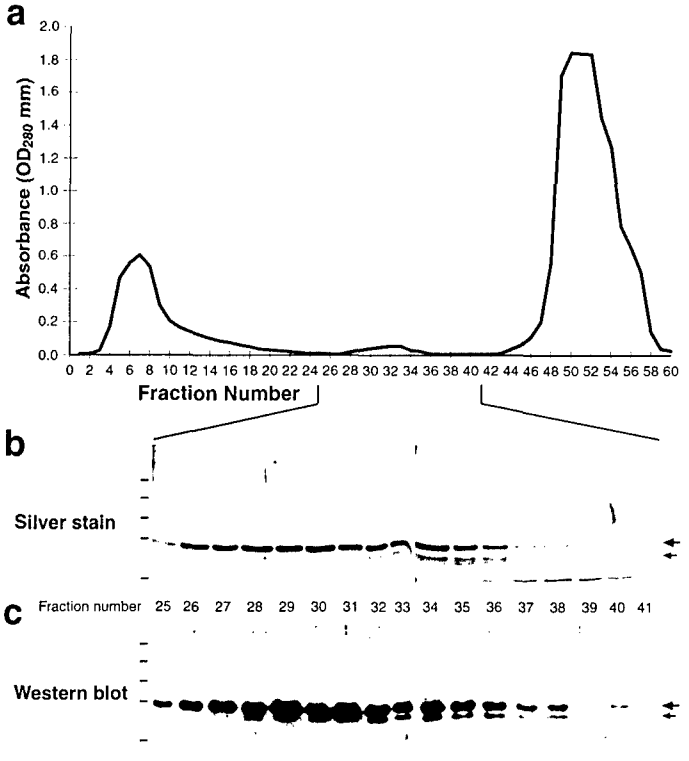

Figure 5. Purification of C-terminal-truncated CRIPTO protein from culture media of baculovirus-infected insect cells. **a,** Elution profile from Sephadex G-75 gel filtration column, showing UV absorbance plotted

against fraction number. **b,** Silver stained gels of indicated column fractions. **c,** Western blot detection of CRIPTO protein in column fractions shown in (**b**). At right, large arrows mark position of intact C-terminal-truncated CRIPTO protein, while small arrows indicate position of a faster migrating CRIPTO product. The position of pre-stained molecular size standards at 25.4, 20, 14, and 9.3 kDa are indicated at left. Note that the purified C-terminal-truncated CRIPTO protein migrates at approximately 14 kDa relative to these size standards; the calculated molecular weight is 15 kDa, and the measured value by gel filtration is approximately 17 kDa. **Methods.** A *Cripto* cDNA corresponding to the mature protein with C-terminal truncation was cloned into the *pMelBac* transfer vector (Invitrogen), which contains a melittin signal sequence for high-level secretion. This construct was used to prepare high-titer (2 x 10^8 pfu/ml) baculovirus stocks in Sf9 insect cells following the supplied protocol (Invitrogen). For protein purification, High-5 insect cells (Invitrogen) were grown under serum-free conditions (Ex-Cell 405 media; JRH Biosciences), and infected at an MOI of 0.4, followed by culture for 72 h at 27°C. After harvest of culture supernatants, 0.1 mM PMSF, 2 mM EDTA, and 0.8 mM DTT (final concentrations) were added, followed by immediate application to a 2.5 by 120 cm Sephadex G-75 column that had been equilibrated with 50 mM HEPES buffer, pH 6.5, 0.1 mM PMSF, 2 mM EDTA, 0.8 mM DTT, and 150 mM NaCl. Fractions (5 ml) were collected and analyzed on 15% gels by SDS-PAGE, followed by silver staining or Western blotting. The fractions containing intact C-terminal truncated CRIPTO protein (numbers 26 to 29) were concentrated to 300 µl using centrifugal filter concentrators (Millipore).

To demonstrate the activity of our purified CRIPTO protein, we have employed a straightforward assay for CRIPTO activity that has been previously described by Salomon and colleagues [24, 28]. This assay uses HC-11 mammary epithelial cells to measure activation of p42/44 MAP kinase, which undergoes phosphorylation within five minutes of addition of active CRIPTO protein to the culture media [28]. Using this assay for CRIPTO activity, we showed that addition of purified CRIPTO protein resulted in significant MAPK phosphorylation (Fig. 6). As a positive control, we showed that addition of EGF was also effective (Fig 6).

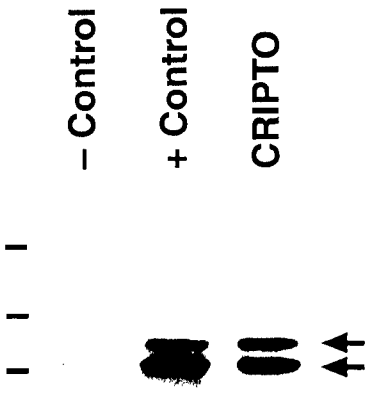

Figure 6. Activity of CRIPTO protein in the MAPK activation assay. Shown is Western blot detection of phosphorylated p42/44 MAPK protein in cell lysates of untreated HC-11 cells (– control), or of HC-11 cells that were treated with EGF (+ control), or with purified CRIPTO protein. Arrows at right indicate positions of phosphorylated MAPK. The position of molecular size standards at 61.5, 50.8, and 37.6 kDa are indicated by dashes at left. **Methods.** The MAPK activation assay was performed as described [24, 28]. We detected p42/44 MAPK phosphorylation in cell lysates of HC-11 cells using a monoclonal antibody that is specific for the phosphorylated protein (New England Biolabs); 150 ng/ml epidermal growth factor (Sigma) was used as a positive control for activation.

(iii) Evidence for an interaction between CRIPTO and NODAL proteins: As a first step for investigating NODAL protein function, we have made constructs that express secreted processed NODAL protein in transfected mammalian cells. For this purpose, we have used a wild-type epitope-tagged *Nodal* construct containing an unmodified prodomain, as well as a chimeric protein with a heterologous BMP-4 prodomain. We have found that processing of unmodified NODAL protein is dependent upon the cell line used for expression, which presumably reflects differential expression of the specific pro-protein convertase(s) required for NODAL processing [29]. Thus, while NODAL protein is not processed successfully in transfected COS cells (data not shown), a cleaved product of the expected size can be found in the culture supernatant of transfected 293T cells (Fig. 7). We are presently seeking to determine whether our secreted NODAL protein displays activity as a dorsalizing factor in frog animal cap assays [30, 31].

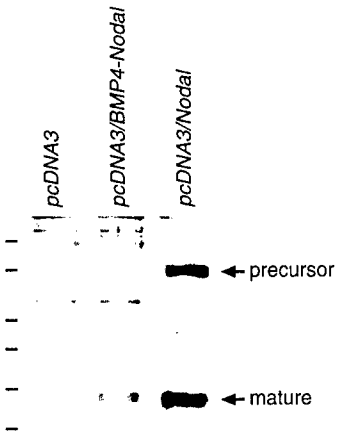

Figure 7. Production of cleaved NODAL protein in mammalian cells. Expression constructs that encode a chimeric BMP4 prodomain fused to the NODAL mature region, or a full-length unmodified NODAL, were FLAG epitope-tagged at their C-terminus. Following transient transfection of 293T cells, culture supernatants were concentrated 10-fold and used for Western blotting with a FLAG antiserum (Sigma). Positions of size standards at 50.3, 37.6, 25.4, 20, 14, and 9.3 kDa are indicated.

Using our purified CRIPTO protein as well as epitope-tagged CRIPTO and NODAL proteins produced in culture supernatants of transfected 293T cells, we have obtained preliminary evidence from co-immunoprecipitation experiments for a direct binding interaction between CRIPTO and NODAL. In the example shown in Fig. 8, we have mixed HA-tagged CRIPTO protein and FLAG-tagged NODAL protein (produced either as a BMP-prodomain chimera or with its native prodomain) in solution, and immunoprecipitated with anti-HA antibody-coupled beads. A specific band corresponding to the mature NODAL product is detected by Western blotting using an anti-FLAG antibody only when both CRIPTO and NODAL proteins are present (Fig. 8). Similar results have been obtained using HA-tagged NODAL and FLAG-tagged CRIPTO proteins, as well as with HA-tagged NODAL and untagged CRIPTO purified from insect cells detected by an anti-CRIPTO antiserum (data not shown). We are currently verifying and extending these results by investigating the interaction of NODAL protein with other members of the EGF-CFC family, and with various mutant forms of CRIPTO. We are also investigating whether a NODAL/CRIPTO protein complex is able to bind to a soluble extracellular domain of ActRIIB, and are attempting to establish a cell culture assay for NODAL activity, using published assays for activin activity.

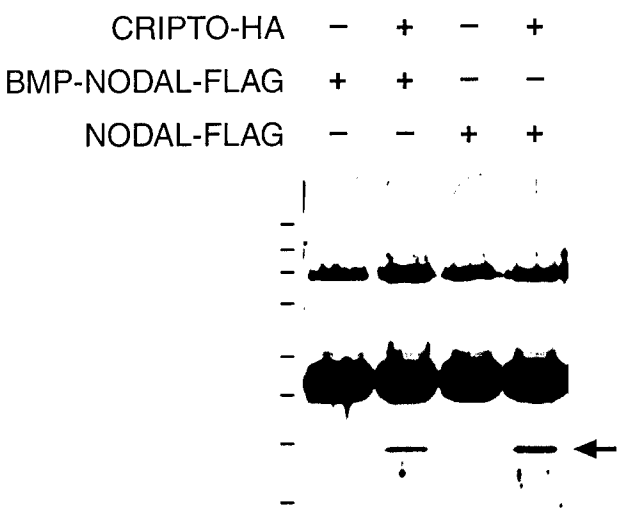

Figure 8. Co-immunoprecipitation of CRIPTO and NODAL proteins. Epitope-tagged CRIPTO-HA and NODAL-FLAG proteins were produced in culture supernatants of transiently transfected 293T cells, followed by 8-fold concentration. Protein complexes were immunoprecipitated by incubation with anti-HA monoclonal antibody-coupled beads (Covance), and washed 4 times with 1x PBS/0.1% NP-40. Immunoprecipitated complexes were resolved on a 12% SDS-PAGE gel and Western blotted using an anti-FLAG monoclonal antibody (Sigma). Positions of size standards at 81.6, 61.5, 50.8, 37.6, 25.4, 20, 14, and 9.3 kDa are indicated.

Our preliminary results suggest that CRIPTO acts as a co-factor for NODAL signaling by a direct protein binding interaction, which presumably mediates signaling through activin receptors. These results imply that CRIPTO may not have a cell-surface receptor, but instead functions solely through interaction with members of the TGF-β family. Thus, we have essentially fulfilled Tasks 13-18 of our Statement of Work.

7. Key Research Accomplishments:

- Analysis of *Cripto* and *Cryptic* mutant phenotypes supports an interaction of *EGF-CFC* genes with the *Nodal* signaling pathway
- Transgenic mice overexpressing *Cripto* in the mammary gland have not displayed an overt morphological phenotype to date, consistent with the lack of activity of *EGF-CFC* genes in isolation, and their function as co-factors for *Nodal.*
- Production of purified CRIPTO protein and mature NODAL protein has led to the preliminary identification of a potential binding interaction between these proteins.

8. Reportable Outcomes:

See attached manuscript in appendix (Yan *et al.* (1999). Genes Dev. *13,* 2527-2537).

9. Conclusions:

In the past year, we have made important progress in investigating the molecular basis of *Cripto* function. We have generated several lines of evidence that *Cripto* acts as an essential co-factor for *Nodal* signaling, and conversely, that *Cripto* activity requires interaction with *Nodal* and possibly other divergent members of the TGF-β family. These results are supported by our preliminary data indicating a direct binding interaction between CRIPTO and NODAL proteins. Taken together, our results have provoked a substantial revision of our views of *Cripto* function, and provide fresh insights into potential mechanisms of *Cripto* activity in mammary development and tumorigenesis.

10. References:

1. Salomon, D.S., Bianco, C., and De Santis, M. (1999). Cripto: a novel epidermal growth factor (EGF)-related peptide in mammary gland development and neoplasia. Bioessays *21,* 61-70.
2. Qi, C.F., Liscia, D.S., Normanno, N., Merlino, G., Johnson, G.R., Gullick, W.J., Ciardiello, F., Saeki, T., Brandt, R., Kim, N., Kenney, N., and Salomon, D.S. (1994). Expression of transforming growth factor alpha, amphiregulin and cripto-1 in human breast carcinomas. Br. J. Cancer *69,* 903-910.
3. Ciardiello, F., Dono, R., Kim, N., Persico, M.G., and Salomon, D.S. (1991). Expression of cripto, a novel gene of the epidermal growth factor gene family, leads to in vitro transformation of a normal mouse mammary epithelial cell line. Cancer Res. *51,* 1051-1054.
4. Shen, M.M., Wang, H., and Leder, P. (1997). A differential display strategy identifies *Cryptic,* a novel EGF-related gene expressed in the axial and lateral mesoderm during mouse gastrulation. Development *124,* 429-442.
5. Ciccodicola, A., Dono, R., Obici, S., Simeone, A., Zollo, M., and Persico, M.G. (1989). Molecular characterization of a gene of the "EGF family" expressed in undifferentiated human NTERA2 teratocarcinoma cells. EMBO J. *8,* 1987-1991.

[redacted] UNPUBLISHED DATA

6. Dono, R., Scalera, L., Pacifico, F., Acampora, D., Persico, M.G., and Simeone, A. (1993). The murine *cripto* gene: expression during mesoderm induction and early heart morphogenesis. Development *118,* 1157-1168.

7. Zhang, J., Talbot, W.S., and Schier, A.F. (1998). Positional cloning identifies zebrafish *one-eyed pinhead* as a permissive EGF-related ligand required during gastrulation. Cell *92,* 241-251.

8. Gritsman, K., Zhang, J., Cheng, S., Heckscher, E., Talbot, W.S., and Schier, A.F. (1999). The EGF-CFC protein one-eyed pinhead is essential for nodal signaling. Cell *97,* 121-132.

9. Ding, J., Yang, L., Yan, Y.T., Chen, A., Desai, N., Wynshaw-Boris, A., and Shen, M.M. (1998). *Cripto* is required for correct orientation of the anterior-posterior axis in the mouse embryo. Nature *395,* 702-707.

10. Yan, Y.-T., Gritsman, K., Ding, J., Burdine, R.D., Corrales, J.D., Price, S.M., Talbot, W.S., Schier, A.F., and Shen, M.M. (1999). Conserved requirement for *EGF-CFC* genes in vertebrate left-right axis formation. Genes Dev. *13,* 2527-2537.

11. Zhou, X., Sasaki, H., Lowe, L., Hogan, B.L., and Kuehn, M.R. (1993). Nodal is a novel TGF-beta-like gene expressed in the mouse node during gastrulation. Nature *361,* 543-547.

12. Conlon, F.L., Lyons, K.M., Takaesu, N., Barth, K.S., Kispert, A., Herrmann, B., and Robertson, E.J. (1994). A primary requirement for nodal in the formation and maintenance of the primitive streak in the mouse. Development *120,* 1919-1928.

13. Massagué, J. (1998). TGF-β signal transduction. Ann. Rev. Biochem *67,* 753-791.

14. Collignon, J., Varlet, I., and Robertson, E.J. (1996). Relationship between asymmetric *nodal* expression and the direction of embryonic turning. Nature *381,* 155-158.

15. Oh, S.P., and Li, E. (1997). The signaling pathway mediated by the type IIB activin receptor controls axial patterning and lateral asymmetry in the mouse. Genes Dev. *11,* 1812-1826.

16. Gu, Z., Nomura, M., Simpson, B.B., Lei, H., Feijen, A., van den Eijnden-van Raaij, J., Donahoe, P.K., and Li, E. (1998). The type I activin receptor ActRIB is required for egg cylinder organization and gastrulation in the mouse. Genes Dev. *12,* 844-857.

17. Waldrip, W.R., Bikoff, E.K., Hoodless, P.A., Wrana, J.L., and Robertson, E.J. (1998). Smad2 signaling in extraembryonic tissues determines anterior-posterior polarity of the early mouse embryo. Cell *92,* 797-808.

18. Nomura, M., and Li, E. (1998). Smad2 role in mesoderm formation, left-right patterning and craniofacial development. Nature *393,* 786-790.

19. Jing, S., Wen, D., Yu, Y., Holst, P.L., Luo, Y., Fang, M., Tamir, R., Antonio, L., Hu, Z., Cupples, R., Louis, J.C., Hu, S., Altrock, B.W., and Fox, G.M. (1996). GDNF-induced activation of the ret protein tyrosine kinase is mediated by GDNFR-alpha, a novel receptor for GDNF. Cell *85,* 1113-1124.

20. Treanor, J.J., Goodman, L., de Sauvage, F., Stone, D.M., Poulsen, K.T., Beck, C.D., Gray, C., Armanini, M.P., Pollock, R.A., Hefti, F., Phillips, H.S., Goddard, A., Moore, M.W., Buj-Bello, A., Davies, A.M., Asai, N., Takahashi, M., Vandlen, R., Henderson, C.E., and Rosenthal, A. (1996). Characterization of a multicomponent receptor for GDNF. Nature *382,* 80-83.

[redacted] UNPUBLISHED DATA

21. de Caestecker, M.P., Parks, W.T., Frank, C.J., Castagnino, P., Bottaro, D.P., Roberts, A.B., and Lechleider, R.J. (1998). Smad2 transduces common signals from receptor serine-threonine and tyrosine kinases. Genes Dev. *12,* 1587-1592.

22. Kretzschmar, M., Doody, J., Timokhina, I., and Massague, J. (1999). A mechanism of repression of TGFbeta/ Smad signaling by oncogenic Ras. Genes Dev. *13,* 804-816.

23. Wang, T.C., Cardiff, R.D., Zukerberg, L., Lees, E., Arnold, A., and Schmidt, E.V. (1994). Mammary hyperplasia and carcinoma in MMTV-cyclin D1 transgenic mice. Nature *369,* 669-671.

24. Kannan, S., De Santis, M., Lohmeyer, M., Riese II, D.J., Smith, G.H., Hynes, N., Seno, M., Brandt, R., Bianco, C., Persico, G., Kenney, N., Normanno, N., Martinez-Lacaci, I., Ciardello, F., Stern, D.F., Gullick, W.J., and Salomon, D.S. (1997). Cripto enhances the tyrosine phosphorylation of Shc and activates mitogen-activated protein kinase (MAPK) in mammary epithelial cells. J. Biol. Chem. *272,* 3330-3335.

25. De Santis, M.L., Kannan, S., Smith, G.H., Seno, M., Bianco, C., Kim, N., Martinez-Lacaci, I., Wallace-Jones, B., and Salomon, D.S. (1997). Cripto-1 inhibits β-casein expression in mammary epithelial cells through a $p21^{ras}$- and phophatidylinositol 3'-kinase-dependent pathway. Cell Growth Diff. *8,* 1257-1266.

26. Storrie, B., and Madden, E.A. (1990). Isolation of subcellular organelles. Meth. Enzymol. *182,* 203-225.

27. Ozols, J. (1990). Preparation of membrane fractions. Meth. Enzymol. *182,* 225-235.

28. De Santis, M.L., Kannan, S., Smith, G.H., Seno, M., Bianco, C., Kim, N., Martinez-Lacaci, I., Wallace-Jones, B., and Salomon, D.S. (1997). Cripto-1 inhibits beta-casein expression in mammary epithelial cells through a p21ras-and phosphatidylinositol 3'-kinase-dependent pathway. Cell Growth Differ. *8,* 1257-1266.

29. Constam, D.B., and Robertson, E.J. (1999). Regulation of bone morphogenetic protein activity by pro domains and proprotein convertases. J. Cell Biol. *144,* 139-149.

30. Jones, C.M., Kuehn, M.R., Hogan, B.L., Smith, J.C., and Wright, C.V. (1995). Nodal-related signals induce axial mesoderm and dorsalize mesoderm during gastrulation. Development *121,* 3651-3662.

31. Piccolo, S., Agius, E., Leyns, L., Bhattacharyya, S., Grunz, H., Bouwmeester, T., and De Robertis, E.M. (1999). The head inducer Cerberus is a multifunctional antagonist of Nodal, BMP and Wnt signals. Nature *397,* 707-710.

Conserved requirement for *EGF–CFC* genes in vertebrate left–right axis formation

Yu-Ting Yan,[1,3] Kira Gritsman,[2,3] Jixiang Ding,[1] Rebecca D. Burdine,[2] JoMichelle D. Corrales,[2] Sandy M. Price,[1] William S. Talbot,[2] Alexander F. Schier,[2,4] and Michael M. Shen[1,4]

[1]Center for Advanced Biotechnology and Medicine (CABM) and Department of Pediatrics, University of Medicine and Dentistry of New Jersey–Robert Wood Johnson Medical School, Piscataway, New Jersey 08854 USA; [2]Developmental Genetics Program, Skirball Institute of Biomolecular Medicine, Department of Cell Biology, New York University School of Medicine, New York, New York 10016 USA

Specification of the left–right (L-R) axis in the vertebrate embryo requires transfer of positional information from the node to the periphery, resulting in asymmetric gene expression in the lateral plate mesoderm. We show that this activation of L-R lateral asymmetry requires the evolutionarily conserved activity of members of the *EGF–CFC* family of extracellular factors. Targeted disruption of murine *Cryptic* results in L-R laterality defects including randomization of abdominal situs, hyposplenia, and pulmonary right isomerism, as well as randomized embryo turning and cardiac looping. Similarly, zebrafish *one-eyed pinhead* (*oep*) mutants that have been rescued partially by mRNA injection display heterotaxia, including randomization of heart looping and pancreas location. In both *Cryptic* and *oep* mutant embryos, L-R asymmetric expression of *Nodal/cyclops*, *Lefty2/antivin*, and *Pitx2* does not occur in the lateral plate mesoderm, while in *Cryptic* mutants *Lefty1* expression is absent from the prospective floor plate. Notably, L-R asymmetric expression of *Nodal* at the lateral edges of the node is still observed in *Cryptic* mutants, indicating that L-R specification has occurred in the node but not the lateral plate. Combined with the previous finding that *oep* is required for *nodal* signaling in zebrafish, we propose that a signaling pathway mediated by *Nodal* and *EGF–CFC* activities is essential for transfer of L-R positional information from the node.

[Key Words: Left–right asymmetry; isomerism; heterotaxia; node; lateral plate mesoderm; *Nodal*]

Received July 14, 1999; revised version accepted August 13, 1999.

Of the three major body axes, the left–right (L-R) axis is the last to be determined during vertebrate embryogenesis. The initial specification of the L-R axis is likely to begin during late stages of gastrulation, but tissue-specific manifestations of morphological L-R asymmetry become apparent much later in development, throughout organogenesis into the late fetal period (for review, see Ramsdell and Yost 1998; Beddington and Robertson 1999). In all vertebrates, the first overt appearance of L-R asymmetry occurs during early somitogenesis, with an initial rightward bending of the linear heart tube that presages the direction of cardiac looping. In the mouse, another early sign of laterality is the direction of embryonic turning that inverts the three primary germ layers of the embryo. Most morphological L-R asymmetry arises at later stages of organogenesis, when unilateral tissues such as the stomach are positioned on one side, or when bilateral paired tissues such as the lung form asymmetrically. Defects in this process of L-R specification can lead to highly pleiotropic effects, including L-R reversals of organ position (inverted situs), mirror image symmetry of bilaterally asymmetric tissues (isomerism), and/or random and independent occurrence of laterality defects in different tissues (heterotaxia).

Recent molecular genetic studies performed in chick, frog, zebrafish, and mouse systems have shown that tissue-specific laterality decisions are mediated by a pathway of regulatory genes that acts during gastrulation and early postgastrulation stages of embryogenesis. These studies have led to a conceptual pathway for L-R axis determination, in which an initial event that breaks L-R symmetry is believed to occur in or around the embryonic node and its derivatives. The resulting L-R positional information is transferred outward to the lateral plate mesoderm, where it is interpreted to generate the situs of individual tissues (for review, see Harvey 1998; Ramsdell and Yost 1998; Beddington and Robertson 1999; King and Brown 1999). Notably, several members of this regulatory pathway are themselves expressed in a

[3]These authors contributed equally to this work.
[4]Corresponding authors.
E-MAIL schier@saturn.med.nyu.edu; FAX (212) 263-7760.
E-MAIL mshen@cabm.rutgers.edu; FAX (732) 235-5318.

L-R asymmetric pattern on the left side of the embryo, in particular the left lateral plate mesoderm.

Several genes in the L-R pathway have roles that appear evolutionarily conserved among vertebrates, including *Nodal* (Levin et al. 1995; Collignon et al. 1996; Lowe et al. 1996; Lustig et al. 1996; Lohr et al. 1997; Sampath et al. 1997; Rebagliati et al. 1998) and *Lefty2* (Meno et al. 1996,1997; Bisgrove et al. 1999; Thisse and Thisse 1999), which encode distant members of the transforming growth factorβ (TGF-β) superfamily, and are asymmetrically expressed in the left lateral plate mesoderm. Another conserved asymmetrically expressed gene is the *Pitx2* homeobox gene, which has been proposed to represent a primary regulator of tissue-specific L-R laterality because it is expressed on the left side of many tissues (Logan et al. 1998; Piedra et al. 1998; Ryan et al. 1998; Yoshioka et al. 1998; Campione et al. 1999). In contrast, there are several apparent differences between vertebrate systems that have complicated our understanding of the L-R pathway. For example, many genes that display transient asymmetry of expression in the chick are not asymmetrically expressed in the mouse, including *activin βB*, *activin receptor IIA*, and *Sonic hedgehog* (*shh*) (Harvey 1998; Ramsdell and Yost 1998; Beddington and Robertson 1999).

We show that L-R axis formation requires the evolutionarily conserved activity of members of the *EGF–CFC* gene family. The *EGF–CFC* family is comprised of mammalian *Cryptic* and *Cripto*, frog *FRL-1*, and zebrafish *one-eyed pinhead* (*oep*) and encodes extracellular proteins containing a divergent EGF-like motif and a novel cysteine-rich CFC motif (Shen et al. 1997; Zhang et al. 1998). We find that targeted disruption of mouse *Cryptic* results in L-R laterality defects including randomization of abdominal situs, pulmonary right isomerism, and vascular heterotaxia, as well as randomized embryo turning and cardiac looping. In parallel studies, we show that partial rescue of *oep* mutant embryos by *oep* mRNA injection results in randomization of the direction of heart looping and location of the pancreas, revealing that loss of *oep* function leads to heterotaxia. Notably, in both *Cryptic* and *oep* mutant embryos, L-R asymmetric gene expression does not occur in the lateral plate mesoderm. Based on recent studies indicating that EGF–CFC proteins act as essential cofactors for Nodal (Gritsman et al. 1999), we propose that a signaling pathway mediated by Nodal and EGF–CFC proteins is required for activation of L-R asymmetric gene expression in the lateral plate mesoderm.

Results

Targeted disruption of Cryptic

Previous mutational analyses have revealed that *oep* and *Cripto* have essential requirements prior to gastrulation (Schier et al. 1997; Ding et al. 1998; Gritsman et al. 1999), but it has been unclear if the later expression of *EGF–CFC* genes reflects a role in postgastrulation processes. In particular, *oep* is expressed in the lateral plate mesoderm and forebrain during early somitogenesis (Zhang et al. 1998), and *Cryptic* is expressed in the lateral plate mesoderm, node, notochordal plate, and prospective floor plate from head-fold stages through approximately the six to eight somite stage (Shen et al. 1997). The expression of *oep* and *Cryptic* is symmetric in the lateral plate and precedes the asymmetric expression of genes such as *Nodal/cyclops*, *Lefty2/antivin* and *Pitx2*.

To determine the biological function of *Cryptic*, we performed targeted gene disruption. The *Cryptic* targeting construct should result in a null mutation, because it deleted most of the third exon and the entire fourth and fifth exons of the gene, which encode two-thirds of the mature protein including the central EGF and CFC motifs (Fig. 1a–c). In addition, a second targeting construct that deleted the entire *Cryptic* coding region resulted in the identical homozygous mutant phenotype (Y.-T. Yan, S.M. Price, and M.M. Shen, unpubl.). Homozygosity for the targeted *Cryptic* mutation resulted in neonatal lethality in the first 2 weeks after birth, apparently because of cardiac defects (see below); to date, only five homozygotes (from >90) have survived past weaning. Our initial indication of a phenotypic defect in L-R laterality was that many newborn *Cryptic* homozygotes displayed a milk spot (corresponding to the stomach) on their right side, instead of the left (Fig. 1d).

L-R laterality defects in Cryptic *mutant mice*

To examine the L-R laterality defects of *Cryptic* homozygous mutant mice, we analyzed their gross anatomy at 18.5 days post coitum (dpc) and at neonatal stages (P0–P7) (Table 1). We found that *Cryptic* homozygotes displayed numerous laterality defects, including heterotaxia, randomization of organ situs, and isomerism of bilaterally asymmetric tissues. Thus, within the abdominal cavity, approximately half of the homozygotes ($n = 22/49$) displayed inverted situs of visceral organs including the stomach, spleen, and pancreas (Fig. 2a,b). In contrast, all homozygous animals displayed asplenia or severe hyposplenia (Fig. 2c–e); a significant proportion of homozygotes also displayed abnormal lobation or midline positioning of the liver (Table 1).

In the thoracic cavity, we found that all homozygotes showed right pulmonary isomerism (Fig. 2f,g); this phenotype is correlated frequently with hyposplenia in human patients with laterality defects (Kosaki and Casey 1998). Moreover, approximately half of the homozygotes ($n = 24/50$) displayed dextrocardia (cardiac apex pointing to the right) or mesocardia (pointing to the middle), as opposed to the normal levocardia (Fig. 2h–j). Regardless of cardiac situs, nearly all homozygotes displayed cardiac abnormalities, most notably transposition of the great arteries (Fig. 2k,l), as well as severe atrial septal defects (Fig. 2m–o). Finally, we observed numerous random and uncorrelated laterality defects within the vasculature, consistent with heterotaxia (Table 1). For example, the azygos vein could be located on the left side (as it is in the wild type), on the right, or bilaterally (Fig. 2p–r).

The L-R laterality defects observed in neonatal *Cryptic*

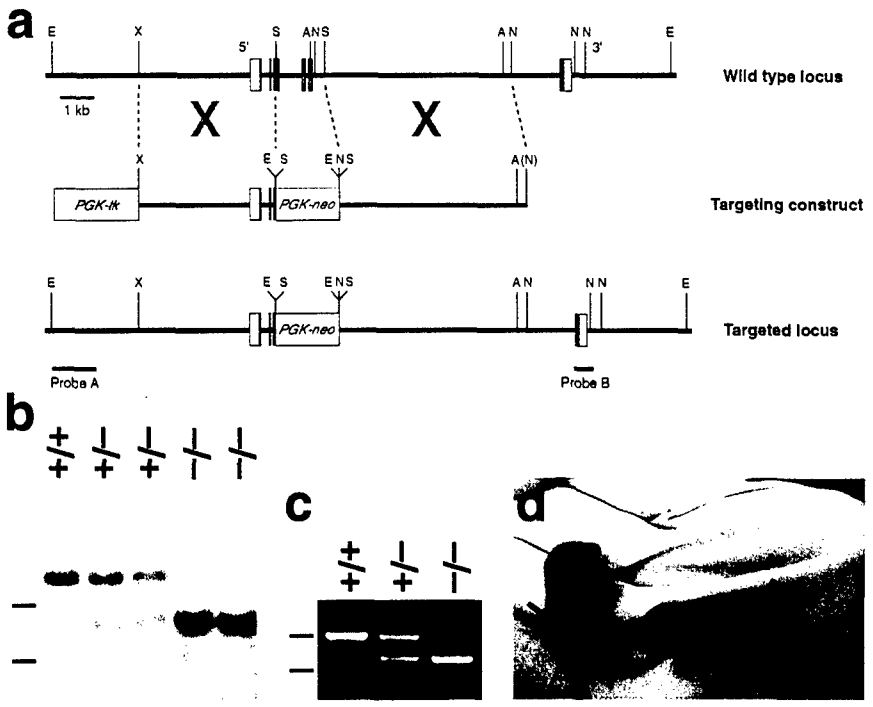

Figure 1. Targeted disruption of *Cryptic*. (*a*) Homologous recombination with the targeting vector results in deletion of exons 4 and 5, as well as most of exon 3; exons are shown as boxes, with the coding region in dark gray. (A) *Avr*II; (E) *Eco*RI; (N) *Nhe*I; (S) *Sma*I; (X) *Xba*I. (*b*) Southern blotting using the 5′-flanking probe. A detects an 18-kb *Eco*RI fragment from the wild-type genomic locus and an 8.5-kb fragment from the targeted allele in progeny of F_1 heterozygous intercrosses; dashes (*left*) indicate positions of markers at 5 and 10 kb. (*c*) PCR analysis of visceral yolk sac DNA from 7.5-dpc embryos, showing amplification of an 860-bp band corresponding to *Cryptic* and a 735-bp fragment corresponding to *neo*; markers at 615 and 861 bp are indicated as above. (*d*) Neonatal mice with milk spots on the right side (−/−) and left side (WT).

homozygotes were paralleled by phenotypic defects observed in early embryogenesis. At 8.5–9.5 dpc, *Cryptic* homozygous embryos were indistinguishable from their wild-type littermates except for randomization of cardiac looping and embryo turning ($n = 21/45$), with these two phenotypes highly correlated (Fig. 2s–u). Because *Cryptic* is expressed in the notochordal plate and prospective floor plate, and laterality defects are frequently associated with node and notochord defects (e.g., Danos and Yost 1996; Dufort et al. 1998; King et al. 1998; Melloy et al. 1998), we investigated potential axial midline defects by skeletal staining of homozygous neonates ($n = 6$), histological sections at 10.5 dpc ($n = 3$), and in situ hybridization with *Shh*, followed by sectioning ($n = 3$). No evidence for axial midline defects was observed (data not shown).

Absence of lateral L-R asymmetric gene expression in Cryptic *mutant embryos*

To determine the basis for L-R patterning defects in *Cryptic* mutants, we performed in situ hybridization on gastrulation and early somite-stage embryos (up to 10 somites), using probes for *Nodal*, *Lefty1*, *Lefty2*, and *Pitx2*, which are asymmetrically expressed at these stages. First, we examined expression of *Lefty1* and *Lefty2*, which are asymmetrically expressed at 2–10 somites in the left prospective floor plate and left lateral plate mesoderm, respectively (Meno et al. 1997, 1998)(Fig. 3a,b,e,f). We found that *Cryptic* homozygous embryos lacked all expression of *Lefty1* ($n = 12$) and *Lefty2* ($n = 9$) at these stages (Fig. 3c,d,g,h); however, an earlier phase of symmetric *Lefty2* expression in newly formed mesoderm during primitive streak stages was un-

Table 1. *Phenotype of* Cryptic *homozygous mice*

Phenotype	Number of mutant/total (%)
Abdominal tissues	
Visceral situs	22/49 inverted (45%)
Spleen	49/49 asplenic/hyposplenic (100%)
Liver	11/27 abnormal (41%)
Abdominal vasculature	
Branching of inferior vena cava	16/25 abnormal (64%)
Position of renal veins	4/19 left anterior (21%)
Thoracic tissues	
Cardiac apex	18/50 dextrocardia, 6/50 mesocardia (48%)
Cardiac malformation	14/16 septal defects (88%); 11/11 transposition of great arteries (100%)
Atrial shape	23/34 right isomerism, 1/34 left (71%)
Lung bronchi	50/50 bilateral eparterial (100%)
Lung lobes	50/50 right isomerism (100%)
Thoracic vasculature	
Aorta relative to pulmonary artery	44/50 aorta ventral, 5/50 adjacent (98%)
Aortic arching	12/29 right (41%)
Position of azygos vein	5/30 right, 6/30 bilateral (37%)
Position of inferior vena cava	4/33 left, 19/33 bilateral (70%)

Phenotypes were scored in mice at 18.5 dpc ($n = 6$) and in neonates at <1 week of age ($n = 44$). Not all phenotypes were scored in each mouse. Unless indicated otherwise in the text, the occurrences of these phenotypes were not noticeably correlated with each other.

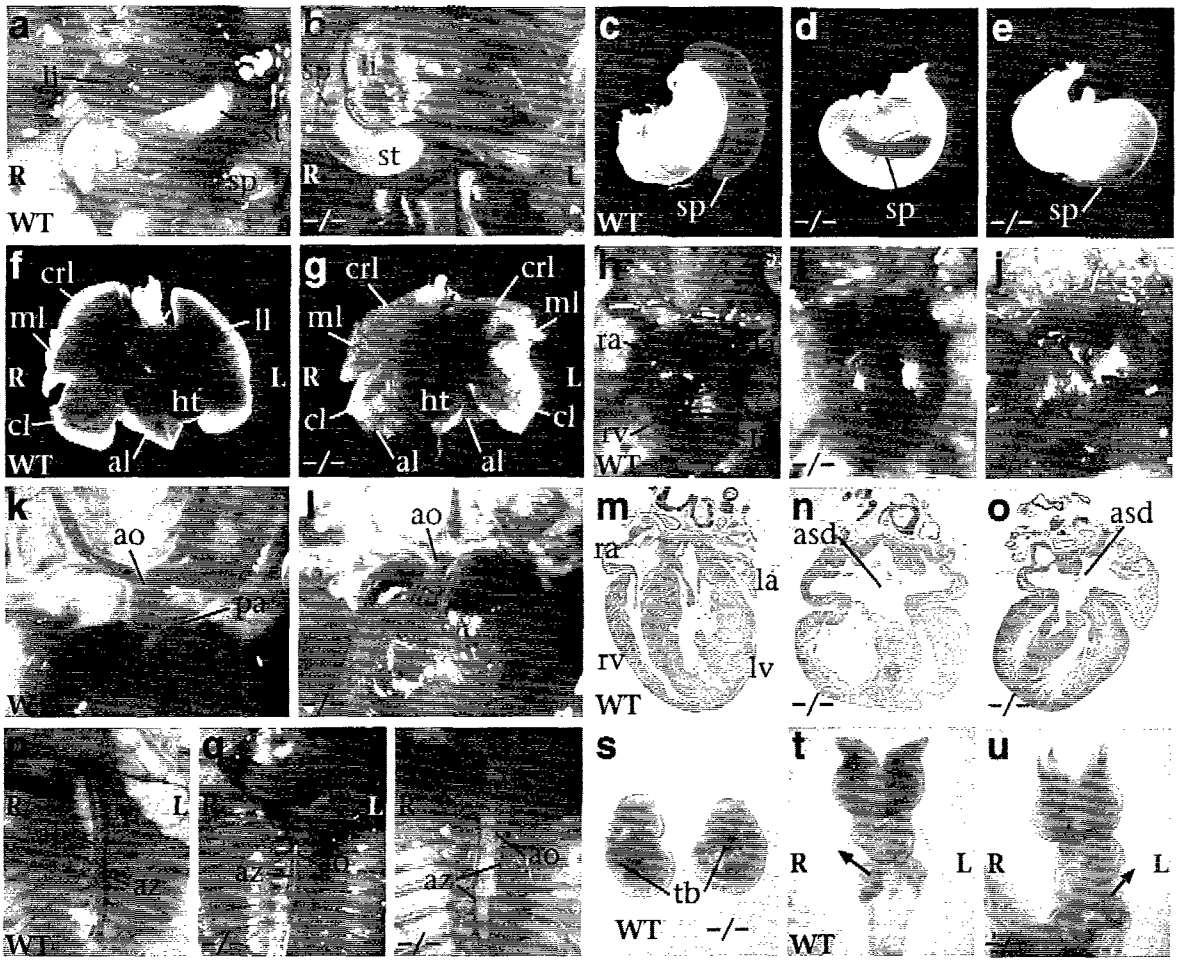

Figure 2. L-R laterality defects in *Cryptic* null mutants. (*a–r*) Ventral views of neonatal mice; in all panels, *left* (*L*) and *right* (*R*) are as indicated. Abdominal cavity of wild type (*a*) and mutant (*b*) with inverted situs and hyposplenia. Stomach and spleen from wild type (*c*), mutant with normal situs (*d*), and mutant with inverted abdominal situs (*e*). Heart and lung lobes of wild type (*f*) and mutant (*g*) with right pulmonary isomerism. Heart positions of wild type with normal levocardia (*h*), and mutants with mesocardia (*i*) and dextrocardia (*j*); note correlation with altered size of the atrial chambers. High-power view of cardiac arterial relationships. In the wild type (*k*), the aorta is dorsal to the pulmonary artery and connects to the left ventricle; in the mutant (*l*), the aorta is ventral and connects to the right ventricle, as shown following injection of blue dye into the right ventricle, consistent with transposition of the great arteries. Sections through hearts of wild type (*m*), and two mutants (*n,o*) that show an atrial septal defect. Position of the azygos vein and direction of aortic arching. In the wild type (*p*), the azygos vein is located on the *left*, and the aorta arches leftward; in the mutant (*q*), the azygos vein crosses over to the *right* and the aorta arches rightward; in the mutant (*r*), there is a bilateral azygos vein while the aorta arches leftward. (*s*) Lateral views of 8.5-dpc embryos, showing altered direction of embryo turning in the mutant. (*t,u*) Ventral views of 10-somite-stage embryos, with arrows indicating direction of cardiac looping in the wild type (*t*) and *Cryptic* mutant (*u*). (al) accessory lobe; (ao) aorta; (asd) atrial septal defect; (az) azygos vein; (cl) caudal lobe; (crl) cranial lobe; (ht) heart; (la) left atrium; (li) liver; (ll) left lung; (lv) left ventricle; (ml) medial lobe; (pa) pulmonary artery; (ra) right atrium; (rv) right ventricle; (sp) spleen; (st) stomach; (tb) tailbud.

affected (data not shown). Next, we examined expression of the homeobox gene *Pitx2*, which is found symmetrically in Rathke's pouch and asymmetrically in the left lateral plate mesoderm and left foregut endoderm from six to eight somites continuing through 9.5 dpc (Ryan et al. 1998; Yoshioka et al. 1998) (Fig. 3i,j). In *Cryptic* mutants at 8.5 and 9.5 dpc ($n = 16$), *Pitx2* expression was still observed in Rathke's pouch but not in the asymmetric domains (Fig. 3k,l).

Finally, we examined expression of *Nodal*, which is found at the lateral boundaries of the node at head-fold and early somite stages, with a transient phase of L-R asymmetry at four to eight somites, and in the left lateral plate mesoderm at approximately two to eight somites (Collignon et al. 1996; Lowe et al. 1996) (Fig. 3m,n). In *Cryptic* mutants ($n = 41$), *Nodal* expression was observed at the lateral boundaries of the node but was never detected in the lateral plate mesoderm (Fig. 3o,p). Notably, the markedly asymmetric expression of *Nodal* at the edges of the node at four to eight somites was still observed in the *Cryptic* mutant embryos ($n = 29$; Fig. 3q–s). Thus, our in situ hybridization results indicate that L-R

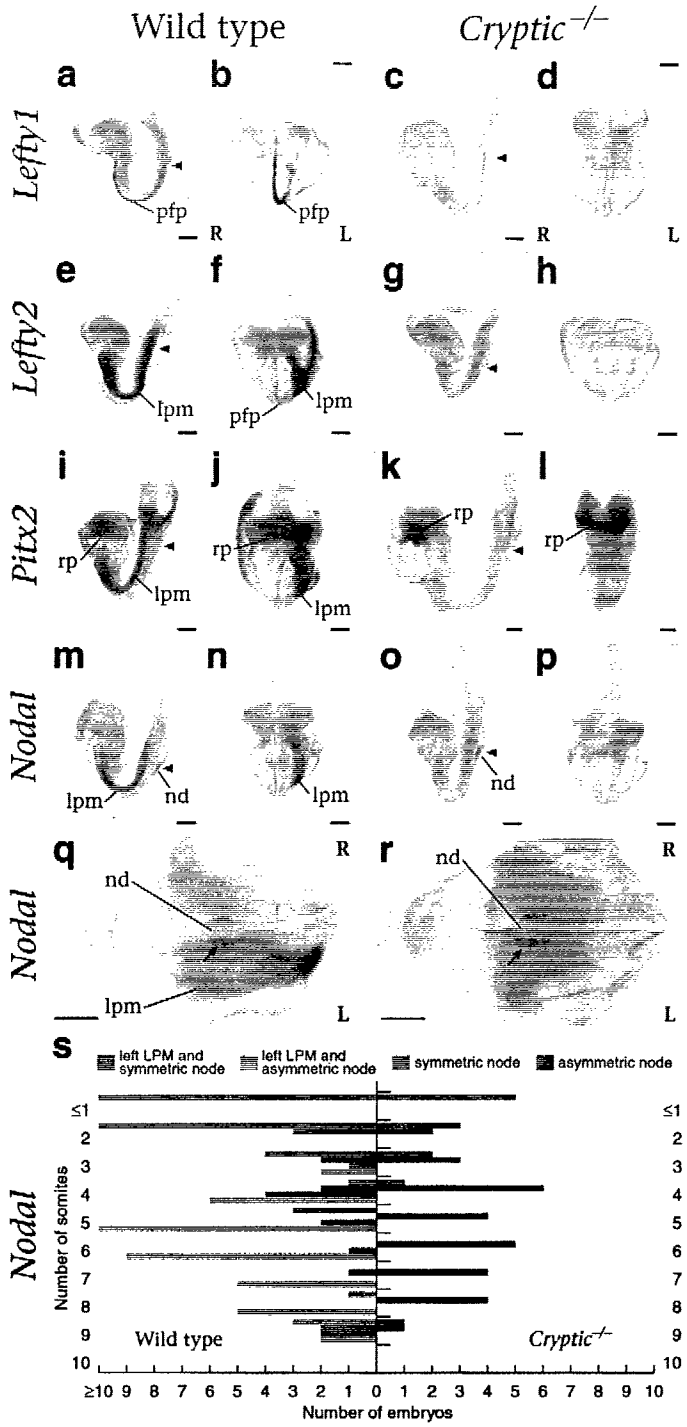

Figure 3. Expression of L-R pathway genes in *Cryptic* homozygous mutant embryos. (*a–p*) Lateral and frontal views of early somite stage mouse embryos following whole-mount in situ hybridization. *Left* (*L*) and *right* (*R*) are as shown, and the position of the node is indicated by an arrowhead. Expression of *Lefty1* is detected in the prospective floor plate of wild type (*a,b*) but not mutant embryos (*c,d*). Expression of *Lefty2* is detected in the left lateral plate mesoderm and weakly in the prospective floor plate of wild type (*e,f*) but not *Cryptic* homozygotes (*g,h*). *Pitx2* expression is observed symmetrically in Rathke's pouch in both wild type (*I,j*) and mutant (*k,l*) embryos, but asymmetric expression in the left lateral plate mesoderm is observed only in the wild type. *Nodal* expression is detected in the node of both wild-type (*m,n*) and mutant (*o,p*) embryos; left lateral plate expression is observed only in the wild type. High-power caudal views of the node in wild-type (*q*) and *Cryptic* homozygote (*r*) show asymmetric expression of *Nodal*. (*s*) Graphical representation of *Nodal* in situ hybridization results. The numbers of wild-type and *Cryptic* mutant embryos analyzed with the indicated *Nodal* expression patterns are graphed according to somite stage. (lpm) lateral plate mesoderm; (nd) node; (pfp) prospective floor plate; (rp) Rathke's pouch.

laterality has been initiated within the node but not in the lateral plate mesoderm.

Heterotaxia in oep *mutant fish*

To determine if the function of *EGF–CFC* genes in L-R determination is conserved in vertebrates, we studied the role of the zebrafish *oep* gene. Previous studies have shown that *oep* is required for formation of mesoderm, endoderm, prechordal plate, and ventral neuroectoderm, correlating with the expression of *oep* in the progenitors of these cell types (Schier et al. 1997; Zhang et al. 1998; Gritsman et al. 1999). During somitogenesis, *oep* is also expressed in the left and right lateral plate, where progenitors of the heart and other organs are located in wild-type embryos (Serbedzija et al. 1998; Zhang et al. 1998). The potential role of *oep* in these territories cannot be analyzed in *oep* mutants, because mutant embryos lack

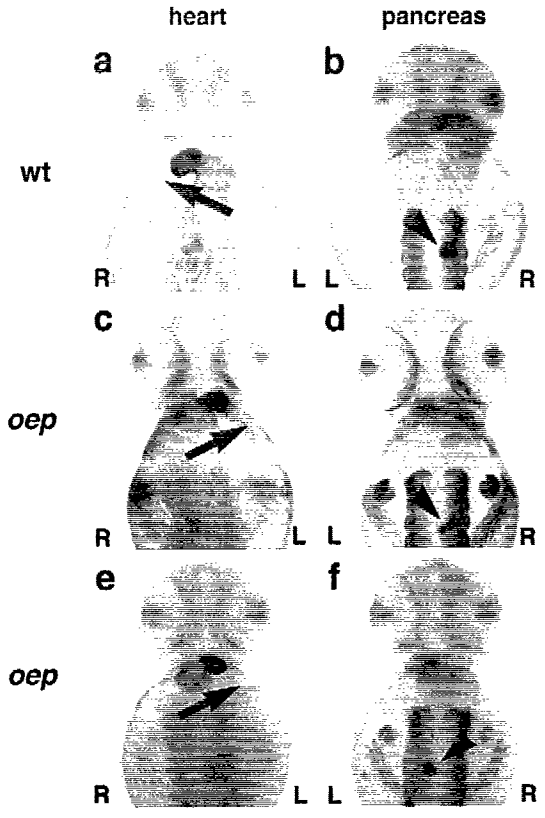

Figure 4. Heart looping and location of the pancreas in *oep* mutants. Ventral (*a,c,e*) and dorsal views (*b,d,f*) of embryos upon immunohistochemistry with MF20 antibody (Bader et al. 1982) and RNA in situ hybridization with *insulin* probe (Milewski et al. 1998); anterior is up. (*a,b*) Wild-type embryo; (*c,d* and *e,f*) two examples of maternal-zygotic *oep* mutant embryos rescued by injection of *oep* mRNA. Note the normal development of eyes and trunk muscle (*d,f*) in rescued embryos [maternal–zygotic *oep* mutants show cyclopia and absence of trunk muscle (Gritsman et al. 1999)]. The arrow indicates heart looping from the atrium (weaker staining, posteriorly) to the ventricle (stronger staining, anteriorly); note right looping in *a* and left looping in *c* and *e*. The arrowhead indicates position of pancreas on *right* (*b,d*) or *left* (*f*) side. We note that the direction of cardiac looping in rescued mutants did not significantly affect their survival to adulthood [50/70 (71%) of right-looping embryos, 46/53 (87%) of left-looping embryos, and 2/6 (33%) of nonlooping embryos survived].

endodermal derivatives and heart (Schier et al. 1997; Gritsman et al. 1999). To circumvent this limitation, we examined the phenotype of maternal–zygotic *oep* (MZ*oep*) embryos whose early defects were rescued by *oep* mRNA injection (Fig. 4). Injected mRNA is present throughout gastrulation (data not shown) and is sufficient to completely rescue the formation of endoderm, mesoderm, axial midline, and ventral neuroectoderm (Fig. 4c–f), but is apparently insufficient to complement the loss of *oep* activity at later stages. Using morphological criteria and marker gene expression, we found that heart and pancreas form, but that the direction of heart looping and the location of the pancreas are randomized with respect to the L-R axis of the embryo (Fig. 4c–f; Table 2). More than 81% (48/59) of *oep* mutant embryos that display abnormal heart asymmetry during embryogenesis survive to adulthood, demonstrating that mRNA injection rescues the development and function of all essential organs. Notably, there was no correlation between abnormal heart asymmetry and the location of the pancreas, revealing that loss of *oep* function leads to heterotaxia.

Absence of L-R asymmetric gene expression in oep *mutants*

To determine the onset of the L-R patterning defect in *oep* mutants, we performed in situ hybridization on somite-stage embryos using probes for *cyclops*, *antivin* (a member of the *lefty* family), and *pitx2*, which are all asymmetrically expressed in the lateral plate mesoderm (Rebagliati et al. 1998; Campione et al. 1999; Thisse and Thisse 1999). Analogous to *Cryptic* mouse mutants, we never detected the normal asymmetric expression of these markers, despite wild-type expression in other regions of the embryo (Fig. 5) . Importantly, asymmetric expression is not initiated, revealing a role for *oep* in the induction of lateral plate asymmetry.

Discussion

Our comparative mutational analyses have shown that homozygous *Cryptic* null mutant mice and partially res-

Table 2. *Direction of heart looping and location of pancreas in wild-type and* oep *mutants*

Genotype: *oep*/+ (+/+ female × −/− male)
Injected mRNA: *lacZ*
Total no. embryos: 96

		Heart (MF20)		
Pancreas (insulin)		L	M	R
R	83 (86.5%)	2 (2.1%)	0	81 (84.3%)
M	6 (6.2%)	0	4 (4.2%)	2 (2.1%)
L	7 (7.3%)	4 (4.2%)	0	3 (3.1%)

Genotype: *oep*/+ (+/+ female × −/− male)
Injected mRNA: *oep*
Total no. embryos: 108

		Heart (MF20)		
Pancreas (insulin)		L	M	R
R	90 (83.3%)	6 (5.5%)	3 (2.8%)	81 (75.0%)
M	4 (3.7%)	2 (1.9%)	0	2 (1.9%)
L	14 (13.0%)	9 (8.3%)	0	5 (4.6%)

Genotype: *oep*/*oep* (−/− female × −/− male)
Injected mRNA: *oep*
Total no. embryos: 106

		Heart (MF20)		
Pancreas (insulin)		L	M	R
R	48 (45.3%)	20 (18.9%)	1 (0.9%)	27 (25.5%)
M	7 (6.6%)	2 (1.9%)	1 (0.9%)	4 (3.8%)
L	51 (48.1%)	26 (24.5%)	1 (0.9%)	24 (22.7%)

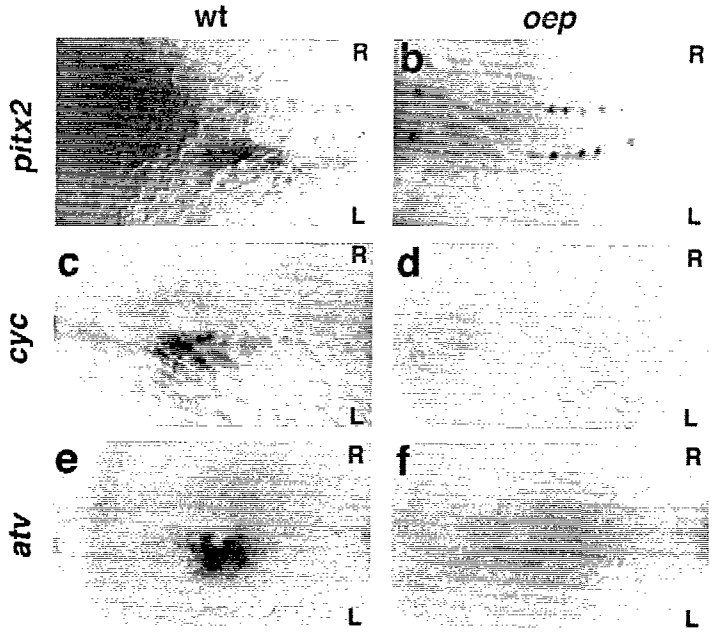

Figure 5. Expression of L-R pathway genes in *oep* mutant embryos. Dorsal view (anterior to the *left*) of 22-somite-stage (*a–d*) and 24-somite-stage (*e,f*) embryos following whole-mount in situ hybridization with *pitx2* (*a,b*), *cyclops* (*c,d*), or *antivin* (*e,f*). Normal expression in the left lateral plate is only detected in wild-type (*a,c*, *oep*/+ embryo injected with *oep* mRNA; *e*, *oep*/+ embryo injected with *lacZ* mRNA) but not in maternal–zygotic *oep* mutants whose early patterning defects were rescued by *oep* mRNA injection (*b*, $n = 58$ embryos analyzed between 14- and 24-somite stages; *d*, $n = 67$; *f*, $n = 44$). Note the normal expression of *pitx2* in the spinal cord (*b*).

cued *oep* mutant fish both display highly penetrant L-R heterotaxia defects. Notably, in *Cryptic* as well as *oep* mutant embryos, *Nodal*, *Lefty2/antivin*, and *Pitx2* are not expressed in the lateral plate mesoderm, indicating that *EGF–CFC* activity is essential for asymmetric gene expression in the lateral mesoderm. Taken together, our findings with *oep* mutant fish are analogous to those for *Cryptic* mutant mice, and establish an evolutionarily conserved requirement for *EGF–CFC* genes in the establishment of L-R asymmetry in vertebrates. Interestingly, this evolutionary conservation of *EGF–CFC* activity in the L-R pathway markedly contrasts with the apparent non-conserved roles of *Fgf8* and *Shh* in the mouse and chick (Meyers and Martin 1999).

Essential function of EGF–CFC *genes in L-R axis specification*

Our results can be readily integrated with a general pathway for L-R axis determination in which initial L-R symmetry is broken in or around the node, and subsequent L-R positional information is transferred to the lateral plate mesoderm (Levin et al. 1995; Logan et al. 1998; Pagan-Westphal and Tabin 1998; Beddington and Robertson 1999). Given the requirement of *oep* activity for *nodal* signaling in zebrafish and the functional conservation of EGF–CFC proteins (Gritsman et al. 1999), we propose that *Cryptic* and *oep* are essential for *Nodal* signaling in L-R axis specification. Our findings indicate that *EGF–CFC* activity is required prior to the activation of L-R asymmetric gene expression in the periphery and may be involved in events downstream from an initial process that breaks L-R symmetry.

Specifically, our results are consistent with two possible models for *EGF–CFC* function in L-R axis formation (Fig. 6). In the first model, *Cryptic/oep* would be required in the lateral plate mesoderm to mediate the response to an asymmetric 'left'-determining signal emanating from the node (Fig. 6a,b). This signal might correspond to Nodal itself, as we have shown previously that EGF–CFC proteins are required for cells to respond to Nodal signals (Gritsman et al. 1999). In this scenario, Nodal signaling from the node or its derivatives cannot be received due to the absence of EGF–CFC activity in the lateral plate.

In the second model for *EGF–CFC* function, *Cryptic/oep* would be required at an earlier stage in the node or its derivatives for the generation or propagation of an asymmetric signal, which could either correspond to Nodal itself or be dependent on Nodal signaling (Fig. 6c). Defects in axial midline structures often result in L-R laterality defects and alterations in asymmetric gene expression, as seen for mouse mutations in *no turning*, *HNF-3β*, *Brachyury*, and *SIL* (Dufort et al. 1998; King et al. 1998; Melloy et al. 1998; Izraeli et al. 1999) and for zebrafish mutations in *no tail* or *floating head* (Danos and Yost 1996; Chen et al. 1997). Although there are no apparent structural defects in the node or its derivatives in *Cryptic* and partially rescued *oep* mutants, absence of EGF–CFC activity might result in a block in Nodal signaling in the axial midline, indirectly leading to defects in the lateral plate (Fig. 6c). Of course, these models are not mutually exclusive, and *Cryptic/oep* may act in both the node and lateral plate. In either case, *EGF–CFC* activity would play an essential role in transferring L-R positional information from the node to the periphery, resulting in asymmetric *Nodal* and *Lefty2/antivin* expression in the lateral plate mesoderm, asymmetric *Lefty1* expression in the mouse floor plate, and subsequent asymmetric *Pitx2* expression, ultimately leading to specification of individual organ situs.

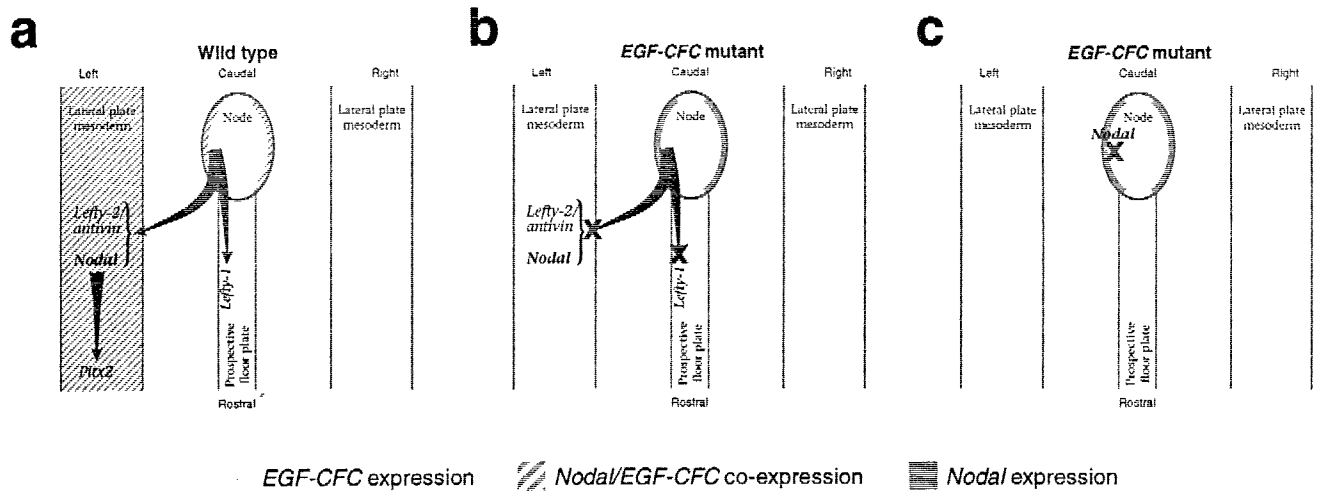

Figure 6. Schematic model for *EGF–CFC* function in L-R axis formation. (*a*) In wild-type embryos, a asymmetric signal emanating from the node activates expression of *Nodal/cyclops* and *Lefty2/antivin* in the left lateral plate mesoderm, as well as *Lefty1* in the left prospective floor plate, leading to subsequent activation of *Pitx2* and specification of organ situs. The node-derived signal could correspond to Nodal itself or to a hypothesized factor downstream of *Shh* signaling that conveys L-R positional information in the chick (Pagan-Westphal and Tabin 1998). (*b*) In this model, the response to the asymmetric node-derived signal is mediated by *Cryptic/oep*, which is symmetrically expressed in the lateral plate mesoderm. In the absence of *EGF–CFC* activity, the lateral plate and prospective floor plate do not respond to the node-derived signal, and asymmetric gene expression fails to occur, resulting in subsequent L-R laterality defects. (*c*) Here, *Cryptic/oep* is required to mediate a *Nodal* activity that is downstream of an initial L-R symmetry-breaking event in or around the node. As a consequence, L-R laterality is specified around the node but fails to be propagated to the lateral plate mesoderm.

Cryptic *mutants as a model for right isomerism/asplenia syndrome*

In humans, the proper L-R situs of the visceral tissues is critical for their morphogenesis and/or physiological function, particularly in the cardiovascular system. In particular, children born with severe heterotaxia generally die shortly after birth, usually due to severe cardiac defects. In many cases, laterality defects in humans that result in heterotaxia can be classified into two primary categories: right isomerism associated with asplenia/hyposplenia and, conversely, left isomerism associated with polysplenia (Goldstein et al. 1998; Kosaki and Casey 1998). Our studies show that *Cryptic* mutant mice recapitulate many features of the right isomerism/asplenia syndrome, suggesting that the *Cryptic* mutant mice may represent a model for a major category of human L-R laterality defects.

Interaction of EGF–CFC genes with the Nodal signaling pathway

In contrast to the phenotype reported here for *oep*, mutations in the zebrafish *nodal* gene *cyclops* do not result in a significant incidence of heart looping defects (Chen et al. 1997). These differing laterality phenotypes of *oep* versus *cyclops* mutants may be due to redundant functions of zebrafish *nodal*-related genes in L-R axis determination. Moreover, a direct requirement for mouse *Nodal* in L-R patterning has also been difficult to establish, due to the early embryonic lethality of *Nodal* mutants, which precludes analysis of later defects. Nonetheless, the L-R phenotypes of *Cryptic* and *oep* mutants, together with the phenotypes of $Nodal^{+/-}$; $HNF\text{-}3B^{+/-}$ and $Nodal^{+/-}$; $Smad2^{+/-}$ mutants (Collignon et al. 1996; Nomura and Li 1998), strongly suggest that Nodal signals are essential for L-R axis specification.

Although the Nodal signaling pathway has not been analyzed at the biochemical level, loss- and gain-of-function studies in mouse, frog, and fish suggest that during gastrulation Nodal signals may act via activin-like receptors (Hemmati-Brivanlou and Melton 1992; Armes and Smith 1997; Chang et al. 1997; New et al. 1997; Oh and Li 1997; Gu et al. 1998; Gritsman et al. 1999; Meno et al. 1999) and the transcription factor Smad2 (Baker and Harland 1996; Graff et al. 1996; Nomura and Li 1998; Waldrip et al. 1998; Weinstein et al. 1998). During germ-layer formation, Nodal signaling has also been shown to be dependent on EGF–CFC activity (Gritsman et al. 1999) and to be antagonized by members of the *Lefty* family (Bisgrove et al. 1999; Meno et al. 1999; Thisse and Thisse 1999). Therefore, it is thought that during gastrulation, Nodal signals are dependent on EGF–CFC proteins to activate activin-like receptors and Smad2, leading to the induction of *Lefty* genes and the attenuation of Nodal signaling.

Comparison of the L-R phenotypes of *Cryptic* and *oep* mutants with the defects found in *Lefty1* and *ActRIIB* mutant mice extends this model to L-R axis determination, raising the possibility that EGF–CFC proteins act universally as essential cofactors for Nodal signaling. First, mice lacking *Lefty1* (Meno et al. 1998) frequently display left pulmonary isomerism and bilateral expression of *Nodal*, *Lefty2*, and *Pitx2*. In contrast, *Cryptic*

mutants display right pulmonary isomerism and lack asymmetric gene expression in the lateral plate mesoderm. These opposing phenotypes support the notion that *Lefty1* acts by antagonizing EGF–CFC dependent *Nodal* activity during L-R determination. Secondly, the phenotype of *Cryptic* mutants superficially resembles that of *ActRIIB* mutant mice, which display right pulmonary isomerism and severe cardiac defects (Oh and Li 1997). Moreover, although *Smad2* homozygotes display early embryonic lethality due to defective specification of the anteroposterior (AP) axis (Nomura and Li 1998; Waldrip et al. 1998; Weinstein et al. 1998), a significant percentage of $Nodal^{+/-}$; $Smad2^{+/-}$ compound heterozygotes display L-R laterality defects (Nomura and Li 1998), which are similar to those of *Cryptic* mutants. The greater severity of the laterality defects in *Cryptic* mice relative to those of *ActRIIB* mutants may reflect the ability of Nodal in conjunction with EGF–CFC proteins to signal through a type II receptor that is partially redundant with ActRIIB, perhaps ActRIIA (also known as ActRII). In summary, these findings indicate that Nodal signaling during L-R development is mediated by EGF–CFC proteins, activin receptors, and Smad2.

Conservation of EGF–CFC function in embryonic axis formation

The phenotypes of *Cripto* and *Cryptic* mutations in mice bear remarkable similarity to those of mutant zebrafish with different timing of *oep* activity. Specifically, complete removal of both maternal and zygotic *oep* activity (MZ*oep* mutants) results in loss of head and trunk mesoderm, endoderm, and an incorrectly positioned AP axis (Gritsman et al. 1999), a phenotype similar to that of *Cripto* mutant mice (Ding et al. 1998). Conversely, restoration of early *oep* activity to MZ*oep* embryos by *oep* mRNA injection rescues these defects, but the insufficient persistence of injected mRNA results in a subsequent L-R laterality defect that strongly resembles the phenotype of *Cryptic* mutants. Taken together, our results indicate that a Nodal and EGF–CFC signaling pathway is essential for both the AP and L-R axes in vertebrates, with the dual role for *oep* in both processes in fish being divided between the related genes *Cripto* and *Cryptic* in mice.

Materials and methods

Gene targeting

A murine *Cryptic* cDNA was used to screen a λFIXII library constructed from 129Sv/J genomic DNA (Stratagene), resulting in the isolation of a 21-kb genomic clone containing the entire coding region. To construct a targeting vector for *Cryptic*, a 3.5-kb *Xba*I–*Sma*I 5′ flank was subcloned into the *Xba*I–*Sma*I sites of *pTKLNL* (Mortensen 1999), followed by subcloning of a 5.0-kb *Sma*I–*Nhe*I 3′ flank, such that the *PGK–neo* and *PGK–tk* cassettes are in the opposite transcriptional orientation to *Cryptic*. Targeting was performed using TC1 ES cells (Deng et al. 1996), with targeted clones obtained at a frequency of 5% (4/88); ES cell culture and blastocyst injection were performed as described previously (Ding et al. 1998). Chimeric males obtained following blastocyst injection were bred with Black Swiss females (Taconic), and germ-line transmission was obtained from one targeted ES clone; two independent lines were also derived using a different targeting vector (Y.-T. Yan, S.M. Price, and M.M. Shen, unpubl.). These targeted *Cryptic* mutations have been maintained through backcrossing with outbred Black Swiss mice; the phenotype appears similar in each line. In addition, the homozygous phenotype appears similar in a hybrid 129/SvEvTac-C57BL/6J strain background.

Mouse genotyping and phenotypic analysis

Genotyping was performed by Southern blotting or by PCR using genomic DNA prepared from tails or embryonic visceral yolk sac. Primers for genotyping were as follows: for wild-type *Cryptic*, 5′GGAGATGGTGCCAGAGAAGTCAGC3′ and 5′AATAGGCAGGGCACACGCAGAAAC3′; for *neo*, 5′CTGCCGCGCTGTTCTCCTCTTCCT3′ and 5′ACACCCAGCCGGCCACAGTCG3′. The presence of cardiac septal defects and transposition of the great arteries was scored by injection of bromphenol blue dye into the right ventricle (Oh and Li 1997), and ventriculoarterial alignment was confirmed by histological sectioning. Cardiac histology was performed by hematoxylin-eosin staining of paraffin sections, with attention given to L-R orientation of sections. Whole-mount in situ hybridization to mouse embryos was performed as described (Ding et al. 1998), using probes for murine *Lefty1* (Meno et al. 1997), *Lefty2* (Meno et al. 1997), *Nodal* (Lowe et al. 1996), and *Pitx2* (Lanctèt et al. 1999).

Zebrafish genetics and phenotypic analysis

Homozygous oep^{tz57}/oep^{tz57} adults were obtained by rescue of homozygous oep^{tz57}/oep^{tz57} embryos with *oep* mRNA (Zhang et al. 1998; Gritsman et al. 1999). To rescue the early patterning defects of *oep* mutants, maternal-zygotic oep^{tz57}/oep^{tz57} embryos were injected with 25–50 pg of *oep* mRNA at the one- to four- cell stage. Heart looping was scored in live embryos and by immunohistochemistry using the MF20 antibody (Bader et al. 1982) that recognizes a myosin heavy chain. Embryos were then processed for in situ hybridization using an *insulin* antisense RNA probe (Milewski et al. 1998). Whole-mount in situ hybridization for *cyclops*, *antivin*, and *Pitx2* was performed as described (Zhang et al. 1998). Zebrafish *pitx2* was cloned by screening of a cDNA library (kindly provided by B. Appel and J. Eisen, University of Oregon, Eugene) with a PCR-amplified *pitx2* homeobox probe (R.D. Burdine; A.F. Schier, and W.S. Talbot, GenBank accession nos. AF156905 and AF156906).

Acknowledgments

We thank Anukampa Barth, Jacques Drouin, Hiroshi Hamada, Yoshiyuki Imai, Michael Kuehn, Rick Mortensen, Cliff Tabin, Bernard Thisse, Christine Thisse, and Steve Wilson for gifts of probes and reagents. We also thank Nishita Desai, Rory Feeney, Elizabeth Heckscher, and Magdalena Michalski for technical assistance. We are particularly grateful to Cory Abate-Shen, Robert Cardiff, and Cliff Tabin for helpful discussions and comments on the manuscript. This work was supported by postdoctoral fellowships from the American Heart Association (J.D.) and Damon Runyon–Walter Winchell Cancer Research Fund (R.D.B.), and by grants from the National Science Foundation (M.M.S.), the American Heart Association (M.M.S.), the U.S.

Army Breast Cancer Research Program (M.M.S.), and the National Institutes of Health (W.S.T., A.F.S., M.M.S.). A.F.S. is a Scholar of the McKnight Endowment Fund for Neuroscience.

The publication costs of this article were defrayed in part by payment of page charges. This article must therefore be hereby marked 'advertisement' in accordance with 18 USC section 1734 solely to indicate this fact.

References

Armes, N.A. and J.C. Smith. 1997. The ALK-2 and ALK-4 activin receptors transduce distinct mesoderm-inducing signals during early Xenopus development but do not cooperate to establish thresholds. *Development* **124:** 3797–3804.

Bader, D., T. Masaki, and D.A. Fischman. 1982. Immunochemical analysis of myosin heavy chain during avian myogenesis in vivo and in vitro. *J. Cell Biol.* **95:** 763–770.

Baker, J.C. and R.M. Harland. 1996. A novel mesoderm inducer, Madr2, functions in the activin signal transduction pathway. *Genes & Dev.* **10:** 1880–1889.

Beddington, R.S.P. and E.J. Robertson. 1999. Axis development and early asymmetry in mammals. *Cell* **96:** 195–209.

Bisgrove, B.W., J.J. Essner, and H.J. Yost. 1999. Regulation of midline development by antagonism of *lefty* and *nodal* signaling. *Development* **126:** 3253–3262.

Campione, M., H. Steinbeisser, A. Schweickert, K. Deissler, F. van Bebber, L.A. Lowe, S. Nowotschin, C. Viebahn, P. Haffter, M.R. Kuehn et al. 1999. The homeobox gene *Pitx2*: Mediator of asymmetric left-right signaling in vertebrate heart and gut looping. *Development* **126:** 1225–1234.

Chang, C., P.A. Wilson, L.S. Mathews, and A. Hemmati-Brivanlou. 1997. A Xenopus type I activin receptor mediates mesodermal but not neural specification during embryogenesis. *Development* **124:** 827–837.

Chen, J.N., F.J. van Eeden, K.S. Warren, A. Chin, C. Nusslein-Volhard, P. Haffter, and M.C. Fishman. 1997. Left-right pattern of cardiac BMP4 may drive asymmetry of the heart in zebrafish. *Development* **124:** 4373–4382.

Collignon, J., I. Varlet, and E.J. Robertson. 1996. Relationship between asymmetric *nodal* expression and the direction of embryonic turning. *Nature* **381:** 155–158.

Danos, M.C. and H.J. Yost. 1996. Role of notochord in specification of cardiac left-right orientation in zebrafish and Xenopus. *Dev. Biol.* **177:** 96–103.

Deng, C., A. Wynshaw-Boris, F. Zhou, A. Kuo, and P. Leder. 1996. Fibroblast growth factor receptor 3 is a negative regulator of bone growth. *Cell* **84:** 911–921.

Ding, J., L. Yang, Y.T. Yan, A. Chen, N. Desai, A. Wynshaw-Boris, and M.M. Shen. 1998. *Cripto* is required for correct orientation of the anterior-posterior axis in the mouse embryo. *Nature* **395:** 702–707.

Dufort, D., L. Schwartz, K. Harpal, and J. Rossant. 1998. The transcription factor HNF3beta is required in visceral endoderm for normal primitive streak morphogenesis. *Development* **125:** 3015–3025.

Goldstein, A.M., B.S. Ticho, and M.C. Fishman. 1998. Patterning the heart's left-right axis: From zebrafish to man. *Dev. Genet.* **22:** 278–287.

Graff, J.M., A. Bansal, and D.A. Melton. 1996. Xenopus Mad proteins transduce distinct subsets of signals for the TGF beta superfamily. *Cell* **85:** 479–487.

Gritsman, K., J. Zhang, S. Cheng, E. Heckscher, W.S. Talbot, and A.F. Schier. 1999. The EGF-CFC protein one-eyed pinhead is essential for nodal signaling. *Cell* **97:** 121–132.

Gu, Z., M. Nomura, B.B. Simpson, H. Lei, A. Feijen, J. van den Eijnden-van Raaij, P.K. Donahoe, and E. Li. 1998. The type I activin receptor ActRIB is required for egg cylinder organization and gastrulation in the mouse. *Genes & Dev.* **12:** 844–857.

Harvey, R.P. 1998. Links in the left/right axial pathway. *Cell* **94:** 273–276.

Hemmati-Brivanlou, A. and D.A. Melton. 1992. A truncated activin receptor inhibits mesoderm induction and formation of axial structures in Xenopus embryos. *Nature* **359:** 609–614.

Izraeli, S., L.A. Lowe, V.L. Bertness, D.J. Good, D.W. Dorward, I.L. Kirsch, and M.R. Kuehn. 1999. The *SIL* gene is required for mouse embryonic axial development and left-right specification. *Nature* **399:** 691–694.

King, T., R.S.P. Beddington, and N.A. Brown. 1998. The role of the *brachyury* gene in heart development and left-right axis specification in the mouse. *Mech. Dev.* **79:** 29–37.

King, T. and N.A. Brown. 1999. Embryonic asymmetry: The left side gets all the best genes. *Curr. Biol.* **9:** R18–R22.

Kosaki, K. and B. Casey. 1998. Genetics of human left-right axis malformations. *Sem. Cell Dev. Biol.* **9:** 89-99.

Lanctèt, C., A. Moreau, M. Chamberland, M.L. Tremblay, and J. Drouin. 1999. Hindlimb patterning and mandible development require the Ptx1 gene. *Development* **126:** 1805–1810.

Levin, M., R.L. Johnson, C.D. Stern, M. Kuehn, and C. Tabin. 1995. A molecular pathway determining left-right asymmetry in chick embryogenesis. *Cell* **82:** 803–814.

Logan, M., S.M. Pagan-Westphal, D.M. Smith, L. Paganessi, and C.J. Tabin. 1998. The transcription factor Pitx2 mediates situs-specific morphogenesis in response to left-right asymmetric signals. *Cell* **94:** 307–317.

Lohr, J.L., M.C. Danos, and H.J. Yost. 1997. Left-right asymmetry of a nodal-related gene is regulated by dorsoanterior midline structures during Xenopus development. *Development* **124:** 1465–1472.

Lowe, L.A., D.M. Supp, K. Sampath, T. Yokoyama, C.V. Wright, S.S. Potter, P. Overbeek, and M.R. Kuehn. 1996. Conserved left-right asymmetry of nodal expression and alterations in murine situs inversus. *Nature* **381:** 158–161.

Lustig, K.D., K. Kroll, E. Sun, R. Ramos, H. Elmendorf, and M.W. Kirschner. 1996. A Xenopus nodal-related gene that acts in synergy with noggin to induce complete secondary axis and notochord formation. *Development* **122:** 3275–3282.

Melloy, P.G., J.L. Ewart, M.F. Cohen, M.E. Desmond, M.R. Kuehn, and C.W. Lo. 1998. No turning, a mouse mutation causing left-right and axial patterning defects. *Dev. Biol.* **193:** 77–89.

Meno, C., Y. Saijoh, H. Fujii, M. Ikeda, T. Yokoyama, M. Yokoyama, Y. Toyoda, and H. Hamada. 1996. Left-right asymmetric expression of the TGF beta-family member lefty in mouse embryos. *Nature* **381:** 151–155.

Meno, C., Y. Ito, Y. Saijoh, Y. Matsuda, K. Tashiro, S. Kuhara, and H. Hamada. 1997. Two closely-related left-right asymmetrically expressed genes, lefty-1 and lefty-2: Their distinct expression domains, chromosomal linkage and direct neuralizing activity in Xenopus embryos. *Genes Cells* **2:** 513–524.

Meno, C., A. Shimono, Y. Saijoh, K. Yashiro, K. Mochida, S. Ohishi, S. Noji, H. Kondoh, and H. Hamada. 1998. lefty-1 is required for left-right determination as a regulator of lefty-2 and nodal. *Cell* **94:** 287–297.

Meno, C., K. Gritsman, S. Ohishi, Y. Ohfuji, E. Heckscher, K. Mochida, A. Shimono, H. Kondoh, W.S. Talbot, E.J. Robertson et al. 1999. Mouse *Lefty-2* and zebrafish *antivin* are feed-

back inhibitors of *Nodal* signaling during vertebrate gastrulation. *Mol. Cell* (in press).

Meyers, E.N. and G.R. Martin. 1999. Differences in left-right axis pathways in mouse and chick: Functions of FGF8 and SHH. *Science* **285:** 403–406.

Milewski, W.M., S.J. Duguay, S.J. Chan, and D.F. Steiner. 1998. Conservation of PDX-1 structure, function, and expression in zebrafish. *Endocrinology* **139:** 1440–1449.

Mortensen, R. 1999. Gene targeting by homologous recombination. In *Current protocols in molecular biology* (ed. F.M. Ausubel, R. Brent, R.E. Kingston, D.D. Moore, J.G. Seidman, J.A. Smith, and K. Struhl), pp. 9.15.11–19.17.13. John Wiley & Sons, New York, NY.

New, H.V., A.L. Kavka, J.C. Smith, and J.B. Green. 1997. Differential effects on Xenopus development of interference with type IIA and type IIB activin receptors. *Mech Dev.* **61:** 175–186.

Nomura, M. and E. Li. 1998. Smad2 role in mesoderm formation, left-right patterning and craniofacial development. *Nature* **393:** 786–790.

Oh, S.P. and E. Li. 1997. The signaling pathway mediated by the type IIB activin receptor controls axial patterning and lateral asymmetry in the mouse. *Genes & Dev.* **11:** 1812–1826.

Pagan-Westphal, S.M. and C.J. Tabin. 1998. The transfer of left-right positional information during chick embryogenesis. *Cell* **93:** 25–35.

Piedra, M.E., J.M. Icardo, M. Albajar, J.C. Rodriguez-Rey, and M.A. Ros. 1998. Pitx2 participates in the late phase of the pathway controlling left-right asymmetry. *Cell* **94:** 319–324.

Ramsdell, A.F. and H.J. Yost. 1998. Molecular mechanisms of vertebrate left-right development. *Trends Genet.* **14:** 459–465.

Rebagliati, M.R., R. Toyama, C. Fricke, P. Haffter, and I.B. Dawid. 1998. Zebrafish nodal-related genes are implicated in axial patterning and establishing left-right asymmetry. *Dev. Biol.* **199:** 261–272.

Ryan, A.K., B. Blumberg, C. Rodriguez-Esteban, S. Yonei-Tamura, K. Tamura, T. Tsukui, J. de la Pena, W. Sabbagh, J. Greenwald, S. Choe et al. 1998. Pitx2 determines left-right asymmetry of internal organs in vertebrates. *Nature* **394:** 545–551.

Sampath, K., A.M. Cheng, A. Frisch, and C.V. Wright. 1997. Functional differences among Xenopus nodal-related genes in left-right axis determination. *Development* **124:** 3293–3302.

Schier, A.F., S.C.F. Neuhauss, K.A. Helde, W.S. Talbot, and W. Driever. 1997. The *one-eyed pinhead* gene functions in mesoderm and endoderm formation in zebrafish and interacts with *no tail*. *Development* **124:** 327–342.

Serbedzija, G.N., J.N. Chen, and M.C. Fishman. 1998. Regulation in the heart field of zebrafish. *Development* **125:** 1095–1101.

Shen, M.M., H. Wang, and P. Leder. 1997. A differential display strategy identifies *Cryptic*, a novel EGF-related gene expressed in the axial and lateral mesoderm during mouse gastrulation. *Development* **124:** 429–442.

Thisse, C. and B. Thisse. 1999. Antivin, a novel and divergent member of the TGFbeta superfamily, negatively regulates mesoderm induction. *Development* **126:** 229–240.

Waldrip, W.R., E.K. Bikoff, P.A. Hoodless, J.L. Wrana, and E.J. Robertson. 1998. Smad2 signaling in extraembryonic tissues determines anterior-posterior polarity of the early mouse embryo. *Cell* **92:** 797–808.

Weinstein, M., X. Yang, C. Li, X. Xu, J. Gotay, and C.X. Deng. 1998. Failure of egg cylinder elongation and mesoderm induction in mouse embryos lacking the tumor suppressor smad2. *Proc. Natl. Acad. Sci.* **95:** 9378–9383.

Yoshioka, H., C. Meno, K. Koshiba, M. Sugihara, H. Itoh, Y. Ishimaru, T. Inoue, H. Ohuchi, E.V. Semina, J.C. Murray et al. 1998. Pitx2, a bicoid-type homeobox gene, is involved in a lefty-signaling pathway in determination of left-right asymmetry. *Cell* **94:** 299–305.

Zhang, J., W.S. Talbot, and A.F. Schier. 1998. Positional cloning identifies zebrafish *one-eyed pinhead* as a permissive EGF-related ligand required during gastrulation. *Cell* **92:** 241–251.

Received
10/29/2001

DEPARTMENT OF THE ARMY
US ARMY MEDICAL RESEARCH AND MATERIEL COMMAND AND FORT DETRICK
810 SCHRIEDER STREET, SUITE 218
FORT DETRICK, MARYLAND 21702-5000

REPLY TO
ATTENTION OF:

MCMR-RMI-S (70-1y) 17 Oct 01

MEMORANDUM FOR Administrator, Defense Technical Information Center (DTIC-OCA), 8725 John J. Kingman Road, Fort Belvoir, VA 22060-6218

SUBJECT: Request Change in Distribution Statement

1. The U.S. Army Medical Research and Materiel Command has reexamined the need for the limitation assigned to technical reports written for grants. Request the limited distribution statements for the Accession Document Numbers listed at enclosure be changed to "Approved for public release; distribution unlimited." These reports should be released to the National Technical Information Service.

2. Point of contact for this request is Ms. Judy Pawlus at DSN 343-7322 or by e-mail at judy.pawlus@det.amedd.army.mil.

FOR THE COMMANDER:

PHYLIS M. RINEHART
Deputy Chief of Staff for
Information Management

Enclosure